Structure-Based Design of "Head-to-Tail" Macrocyclic PROTACs

Chungen Li,[▽] Yihan Chen,[▽] Weixue Huang,[▽] Yudi Qiu, Shengjie Huang, Yang Zhou, Fengtao Zhou, Jian Xu, Xiaomei Ren, Jinwei Zhang, Zhen Wang, Ming Ding, and Ke Ding*
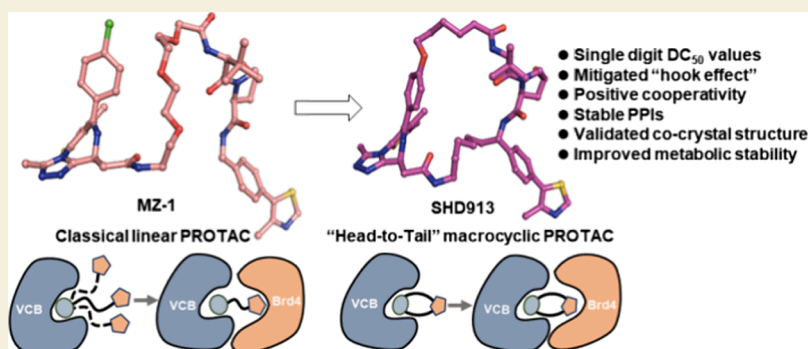
ACCESS | Metrics & More | Article Recommendations | Supporting Information

ABSTRACT: Macrocyclization is a compelling strategy for conventional drug design for improving biological activity, target specificity, and metabolic stability, but it was rarely applied to the design of PROTACs possibly due to the mechanism and structural complexity. Herein, we report the rational design of the first series of "Head-to-Tail" macrocyclic PROTACs. The resulting molecule **SHD913** exhibited pronounced Brd4 protein degradation with low nM DC_{50} values while almost totally dismissing the "hook effect", which is a general character and common concern of a PROTAC, in multiple cancer cell lines. Further biological evaluation revealed that the compound exhibited positive cooperativity and induced *de novo* protein−protein interactions (PPIs) in both biophysical and cellular NanoBRET assays and outperformed macroPROTAC-1 that is the first reported macrocyclic Brd4 PROTAC, in cellular assays. *In vitro* liver microsomal stability evaluation suggested that **SHD913** demonstrated improved metabolic stability in different species compared with the linear counterpart. The co-crystal structure of Brd4[BD2]: **SHD913**: VCB (VHL, Elongin C and Elongin B) complex determination and molecular dynamics (MD) simulation also elucidated details of the chemical-induced PPIs and highlighted the crucial contribution of restricted conformation of **SHD913** to the ternary complex formation. These results collectively support that macrocyclization could be an attractive and feasible strategy for a new PROTAC design.

KEYWORDS: *PROTACs, "head-to-tail" macrocyclization, hook effect, cocrystal structure, ternary complex*

■ INTRODUCTION

Targeted protein degradation (TPD) is emerging as an attractive modality for both drug discovery and chemical biology research because of its "event-driven" action mode and closely mimicking the biologically genetic knockout.[1] More than 30 proteolysis-targeting chimeras (PROTACs), which are bifunctional molecules that trigger protein proteasomal degradation by hijacking them into spatial proximity with an E3 ubiquitin ligase, have been advanced into different stages of clinical development.[2] PROTACs demonstrate significant advantages over conventional drugs, such as a catalytic or substoichiometric pharmacological effect, an extended duration of action, and accessibility for intractable targets.[3] Nonetheless, the theoretical "hook effect" (bell-shaped pharmacology) is a common concern for the PROTAC therapy due to the requirement for E3: PROTAC: target ternary complex formation.[4] A PROTAC molecule generally exhibits a "dumbbell-shaped" geometry, in which a flexible or rigid linear linker is applied to facilitate the formation of the ternary complex.[5] However, conformational flexibility of the linear PROTACs might result in unfavorable pharmacokinetic properties (e.g., poor solubility and metabolic liability), which is another major challenge for PROTAC development.

Macrocyclization is a compelling strategy for conventional drug design to improve potency and drug-likeness of a molecule through conformational restriction, and macrocycles become privileged scaffolds for modulating protein−protein interactions (PPIs) harboring large, flat, and dynamic surfaces.[6] For instance, macrocyclic natural products, i.e., cyclosporin A (CsA),[7]

tacrolimus (FK506),[8] and rapamycin,[9] were defined as the first "molecule glues" in the 1990s because of their capabilities to induce and stabilize PPIs (Figure 1A).[1b,10] Most recently, a
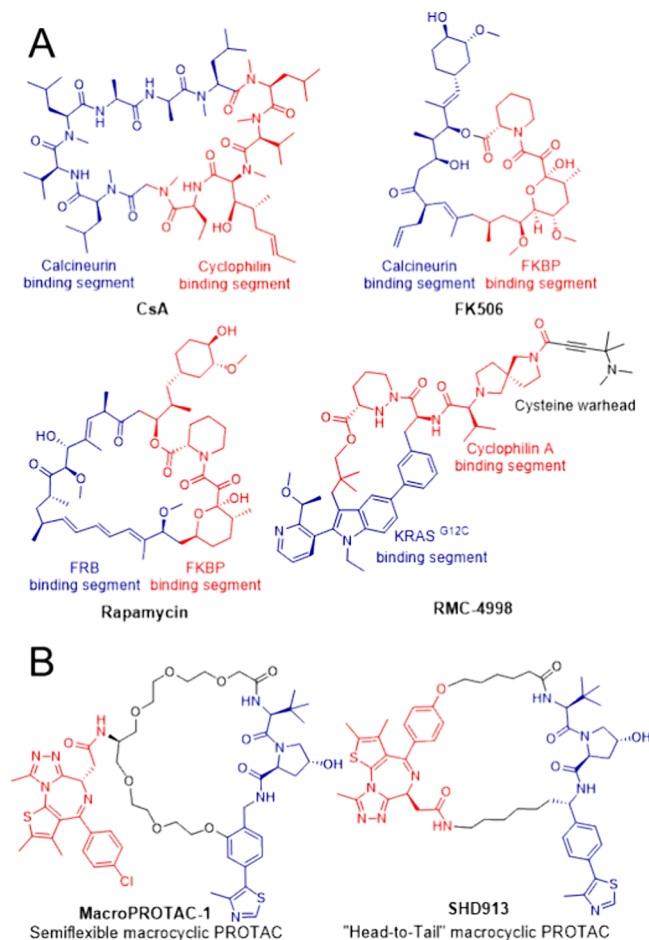

Figure 1. (A) Examples of macrocyclic molecules capable of inducing and/or stabilizing PPIs. (B) Structure of **macroPROTAC-1** and **SHD913**.

synthetic macrocyclic molecule, RMC-4998 (Figure 1A), was also reported to induce PPIs between cyclophilin A and KRAS^{G12C} and achieved promising therapeutic effects in non-small cell lung cancer (NSCLC) models.[11] Given the fact that a PROTAC generally binds to surface pockets of the target protein and E3 ligase, and multiple linking sites could be available in both the warheads and E3 binders. We proposed that macrocyclic derivatives could be designed to lock the molecules in conformation favorable for ternary complex formation by decreasing the molecular entropy. Notably, a semiflexible macrocyclic PROTAC of the bromodomain and extra-terminal motif (BET) protein (Brd4) (**macroPROTAC-1**) was recently reported to exhibit strong target degradation potency. A co-crystal structure of **macroPROTAC-1** bound in a ternary complex with VHL and Brd4^{BD2} was also solved to validate the design rationale,[12] providing the first "proof of concept" for a macrocyclization approach in the new PROTAC design. Whereas the molecule could also be considered as a linear PROTAC harboring a macrocyclic Von Hippel−Lindau (VHL) ligand since the target binding motif is out of the macro-ring system (Figure 1B).

Utilizing VHL-Brd4 as a model system, we conducted structure-based design of the "Head-to-Tail" macrocyclic PROTACs by taking advantage of the pioneering structural information on a ternary complex formed by VHL, the second bromodomain (BD2) of Brd4 (Brd4^{BD2}) and **MZ1**, a Brd4 PROTAC with a linear polyethylene glycol (PEG) linker.[13] The new macrocyclic PROTAC exhibited fast and pronounced degrading potency with low nM DC$_{50}$ values. Strikingly, no measurable "hook effect" was detected for the compound across a panel of cancer cell lines, even at concentrations of approximately 10,000 times greater than the determined DC$_{50}$ values. Further biophysical evaluation and nanoluciferase bioluminescence resonance energy transfer (NanoBRET) determination confirmed that the compound exhibited a positive cooperative effect and induced *neomorphic* PPIs between Brd4^{BD2} and VHL both *in solution* and in cells. The co-crystal structure of the ternary complex was also solved to elucidate detailed interactions among Brd4^{BD2}, VHL, and the PROTAC. To the best of our knowledge, this work represents the first example of a structure-based design of "Head-to-Tail" macrocyclic PROTACs (Figure 1B).

RESULTS AND DISCUSSION

Structure-Based Design of Novel "Head-to-Tail" Macrocyclic PROTACs

Alessio Ciulli and co-workers[13] previously reported a crystal structure of Brd4^{BD2}: **MZ1**: VCB (VHL, Elongin C, and Elongin B) ternary complex (Figure 2A, PDB: 5T35). It was shown that
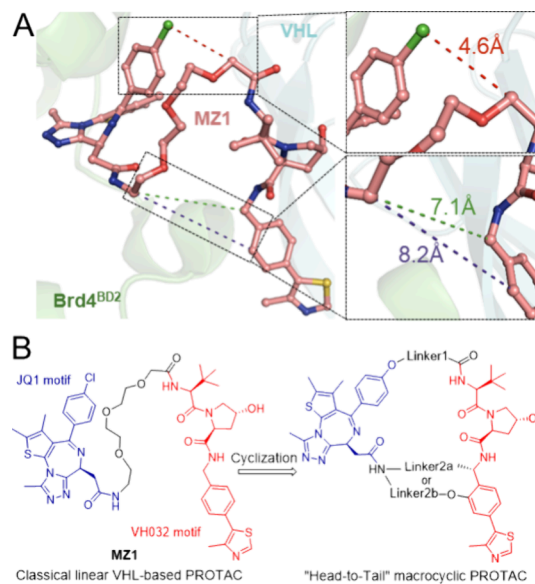

Figure 2. Structure-based design of "Head-to-Tail" macrocyclic PROTACs. (A) Structure feature analysis of the Brd4^{BD2}: **MZ1**: VHL (PDB: 5T35) ternary complex. **MZ1** is shown in salmon sticks. Brd4^{BD2} and VHL are shown in green and cyan cartoon, respectively. (B) Structure-based design of "Head-to-Tail" macrocyclic PROTACs.

MZ1 induced de novo PPIs between the BD2 domain of Brd4 and VHL proteins to form a "bowl-shaped" interface where the molecule was accommodated. The linear PROTAC **MZ1** generally adopted a "Z" conformation in which the JQ1- and VH032- motifs bound with Brd4^{BD2} and VHL (Figure 2A), respectively, in similar modes to the original monovalent ligands.[14] Structural feature analysis revealed that the Cl atom

Scheme 1. Synthesis of Compounds 10a–10i and 15a–15c[a]
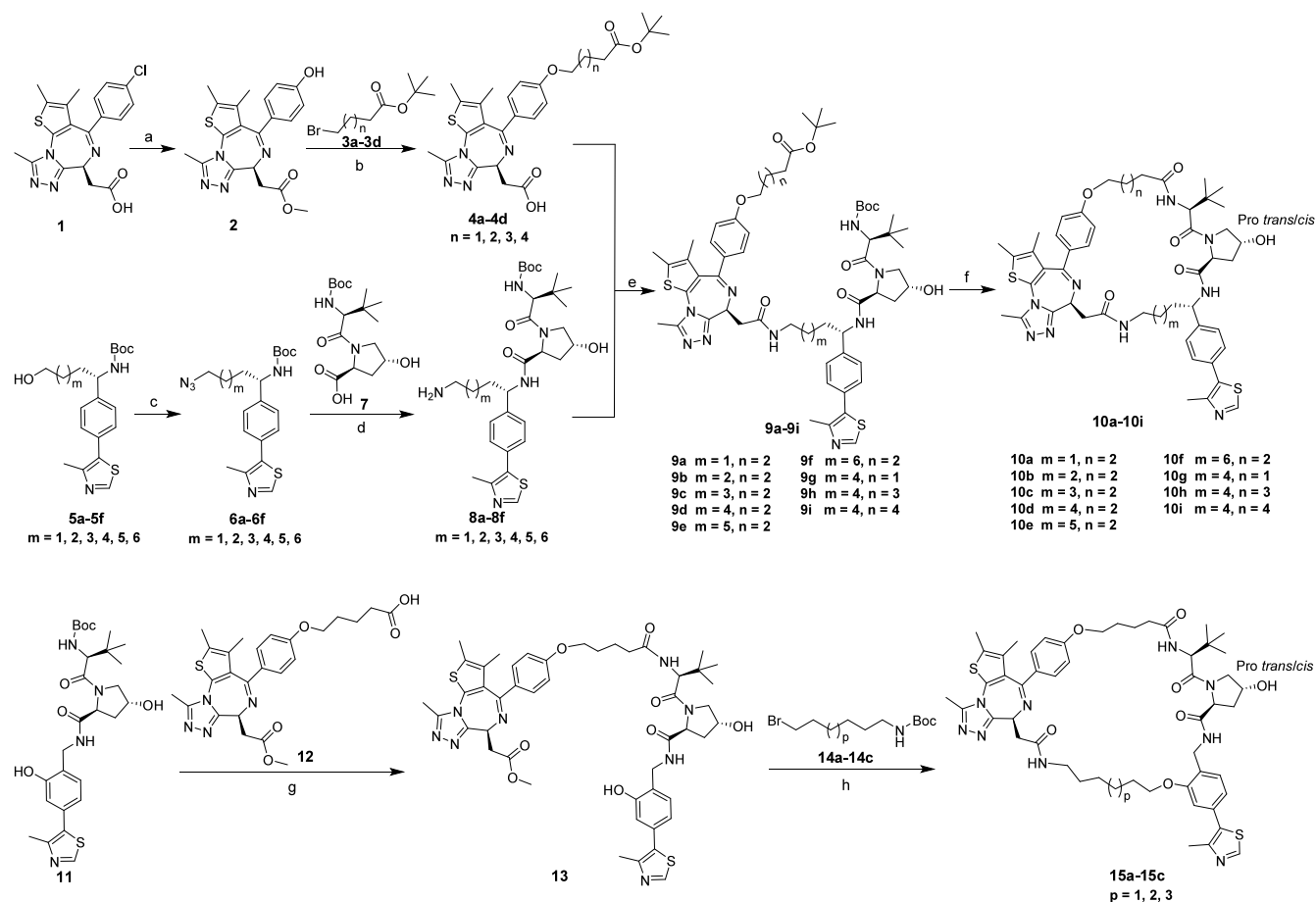
[a]Reagents and conditions: (a) (i) Pd$_2$(dba)$_3$, KOH, tBuBrettPhos, 1,4-dioxane, H$_2$O, 100 °C, 12 h, 86%; (ii) thionyl chloride, methanol, 0 °C to room temperature (RT), 5 h, 95%; (b) (i) potassium carbonate (K$_2$CO$_3$), acetonitrile, 80 °C, 12 h, 80−90%; (ii) lithium hydroxide (LiOH), tetrahydrofuran (THF), H$_2$O, RT, 3−6 h, 90−95%; (c) diphenylphosphoryl azide (DPPA), 1,8-diazabicyclo[5,4,0]undec-7-ene (DBU), anhydrous N,N-dimethylformamide (DMF), anhydrous toluene, 50 °C, 12 h, 80−90%; (d) (i) trifluoroacetic acid (TFA), dichloromethane (CH$_2$Cl$_2$), RT, 3 h; (ii) 2-(7-azabenzotriazol-1-yl)-N',N',N'-tetramethyluronium hexafluorophosphate (HATU), triethylamine (Et$_3$N), DMF, RT, 5 h; (iii) triphenylphosphine, ammonium hydroxide (NH$_3$.H$_2$O), 1,4-dioxane, H$_2$O, RT, 12 h, 40−70% over three steps; (e) HATU, Et$_3$N, DMF, RT, 5 h, 50−70%; (f) (i) TFA, CH$_2$Cl$_2$, RT, 3 h; (ii) HATU, N,N-diisopropylethylamine (DIEA), DMF, RT, 3 h, 50−65% over two steps; (g) (i) TFA, CH$_2$Cl$_2$, RT, 3 h; (ii) HATU, Et$_3$N, DMF, RT, 5 h, 61% over two steps; (h) (i) K$_2$CO$_3$, acetonitrile, 80 °C, 12 h; (ii) LiOH, THF, H$_2$O, RT, 3−5 h; (iii) TFA, CH$_2$Cl$_2$, RT, 3 h; (iv) HATU, DIEA, DMF, RT, 3 h, 30−40% over four steps.
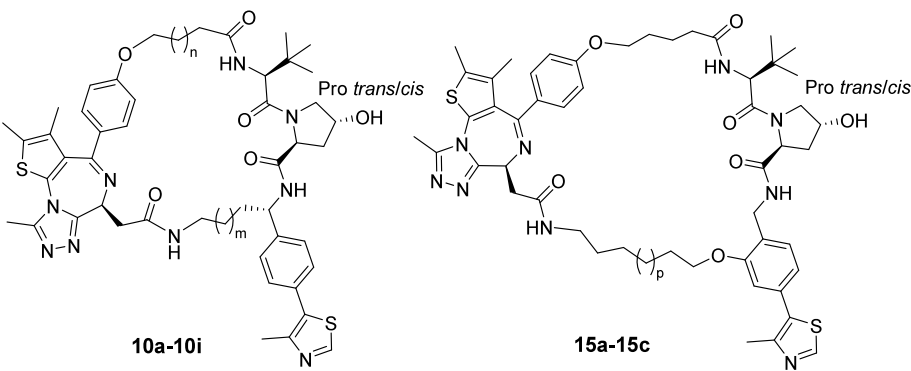
in the warhead orientated to the PPI interface and closely approached the acetyl group of the VH032 moiety with a distance of 4.6 Å, suggesting that it might provide a new position to connect the VHL ligand with a short linker. X-ray structure also showed that the amide of the JQ1- moiety was located toward the benzylic and *ortho*-phenyl positions of the VH032 moiety with distances of 7.1 and 8.2 Å, respectively (Figure 2A). Studies have shown that both benzylic and *ortho*-phenyl positions of VH032 are solvent accessible and feasible to be utilized for VHL-based PROTAC design.[15] Inspired by the structural information, a series of new "Head-to-Tail" macrocyclic PROTACs were designed aiming to decrease binding energy penalty, so the compound would be locked in conformations favorable for the ternary complex formation. Additionally, macrocyclization might also provide opportunities to improve the metabolic stability of the VHL-based PROTACs.[16] Structurally, the macrocyclic molecules harbor two short linkers. One is between the JQ1- phenyl group and the VH032- acetyl moiety (upper, linker1), and the other one is for

linking JQ1- amide with VH032 through benzylic or ortho-phenyl positions (bottom, linker2a, 2b) (Figure 2B).

Chemical Synthesis of the Macrocyclic PROTACs

Synthesis of the designed molecules is depicted in Scheme 1. The JQ1-moieties were prepared from commercially available (S)-2-(4-(4-chlorophenyl)-2,3,9-trimethyl-6H-thieno [3,2-f] [1,2,4] triazolo[4,3-a] [1,4] diazepin-6-yl) acetic acid **1**. A palladium-catalyzed hydroxylation was conducted by utilizing tris(dibenzylideneacetone)dipalladium (Pd$_2$(dba)$_3$) as a catalyst, t-BuBrettPhos as a ligand, and potassium hydroxide (KOH) as a base, and the resulting intermediate was consequently esterified to produce compound **2**.[17] Compound **2** was etherified with bromo-substituted esters **3a**–**3d** and then hydrolyzed to yield **4a**–**4d**. The VHL moieties were synthesized from **5a** to **5f**, which were prepared according to the previously reported procedures.[18] **5a**–**5f** underwent a Mitsunobu reaction to afford azides **6a**–**6f**, which were deprotected and reacted with compound **7** to produce the corresponding amides, in which the azide was further reduced to give primary amines **8a**–**8f**. JQ1-moieties **4a**–**4d** were coupled with **8a**–**8f** to afford **9a**–**9i**,

Table 1. Degradation Efficiency of Compounds 10a−10i and 15a−15c

	linker				% Brd4 degradation (PC-3)[a]	
compds	n	m	p	trans/cis[b]	10 nM (L/S)[c]	100 nM (L/S)
10a	2	1		trans	37/19	63/43
10b	2	2		trans	15/17	84/85
10c	2	3		16/1	45/56	94/94
10d	2	4		7/1	78/84	94/95
10e	2	5		10/1	20/42	92/97
10f	2	6		3/1	36/28	97/96
10g	1	4		3/1	7/0	48/37
10h (SHD913)	3	4		7/1	81/86	95/95
10i	4	4		16/1	85/91	95/97
15a			1	7/3	47/36	89/87
15b			2	7/3	57/40	84/91
15c			3	7/3	59/60	96/95
MZ1					82/95	95/96

[a]Degradation efficiency was determined by immunoblotting determination after treatments with compounds in PC-3 cells for 24 h. The reported values were calculated from two independent determinations. [b]The rate of trans-/cis-conformation was determined by ^{1}H NMR. [c]L represents long Brd4 isoform; S represents short Brd4 isoform.

which were deprotected and followed by a macrocyclization to give the final compounds **10a−10i**.

Compounds **15a−15c** were synthesized from the starting material **11**, which was prepared according to a reported procedure.[19] Deprotection of the Boc group and a subsequent amidation were performed to yield **13**. Compound **13** was reacted with bromo-substituted linkers **14a−14c**, followed by hydrolysis, Boc-group deprotection, and cyclization reaction to yield final compounds **15a−15c**.

^{1}H NMR determination suggested that macrocyclic compounds **10c−10i** and **15a−15c** were obtained with inseparable cis-/trans-rotamers because of the presence of the hydroxyproline restricting the amide bond rotation in the VHL binding moiety.[20] The [1]H−[1]H ROESY spectrum confirmed that the trans-conformation was more stable and the compounds could be converted to a single conformation by heating to 80 °C as determined by ^{1}H NMR (Supporting Information).

Structure-Degradation Relationship (SDR) of the Macrocyclic PROTACs

The structure of Brd4[BD2]: **MZ1**: VCB (PDB: 5T35) ternary complex showed that the distance between the Cl atom and the acetyl group in **MZ1** was 4.6 Å, which is approximately equivalent to three C−C bonds.[13] Therefore, we first designed compounds with 3 −CH₂− units ($n = 2$) as the linker1 and explored the optimal length of linker2a by utilizing the benzylic position as the docking site for macrocyclization. As mentioned above, the macrocycles could adopt inseparable cis-/trans conformations because of the hydroxyproline moiety in the VHL binding motif. The ratios of trans-/cis- rotamers were

reported based on ^{1}H NMR determination. The degradation potency of the compounds was determined by using immunoblotting assays in PC-3 prostate cancer cells at 10 and 100 nM after 24 h treatments, with **MZ1** as a positive control (Table 1). The results showed that most of the new "Head-to-Tail" macrocyclic molecules demonstrated obvious protein degrading potency, and the length of linker2a had a huge impact on the activity (compounds **10a−10f**). Among the first series of molecules, compound **10d** with a 6-CH₂−unit linker2a ($m = 4$) exhibited the strongest potency with degradation rates of 78%/84% and 94%/95% against the long/short forms of Brd4 protein at 10 and 100 nM, respectively. Lengthening or shortening linker2a caused a significant decrease of degradation potency on both long and short forms of Brd4 at 10 nM, although all of the molecules exhibited strong degradation at 100 nM. For instance, the compound with a 4-CH₂−unit linker2a ($m = 2$, **10b**) displayed obviously decreased activity with degradation rates of 15 and 17% against the long and short forms of Brd4 at 10 nM, respectively, while the corresponding numbers are 84 and 85% at a concentration of 100 nM. Compounds with longer linker2a (**10e**, **10f**) also exhibited obviously decreased potencies at 10 nM, although their degradation efficiencies were almost equal to **10d** at 100 nM. After identifying the optimal length of linker2a ($m = 4$), we validated the impact of the length of linker1. It was shown that shorter linker1 ($n = 1$, **10g**) totally abolished the protein degradation potency at low concentrations, while the compounds with longer linker1 ($n = 3$, **10h** (SHD913); $n = 4$, **10i**) exhibited comparable activities to that of **10d** under both low and high concentrations. Notably, compounds **10d**,
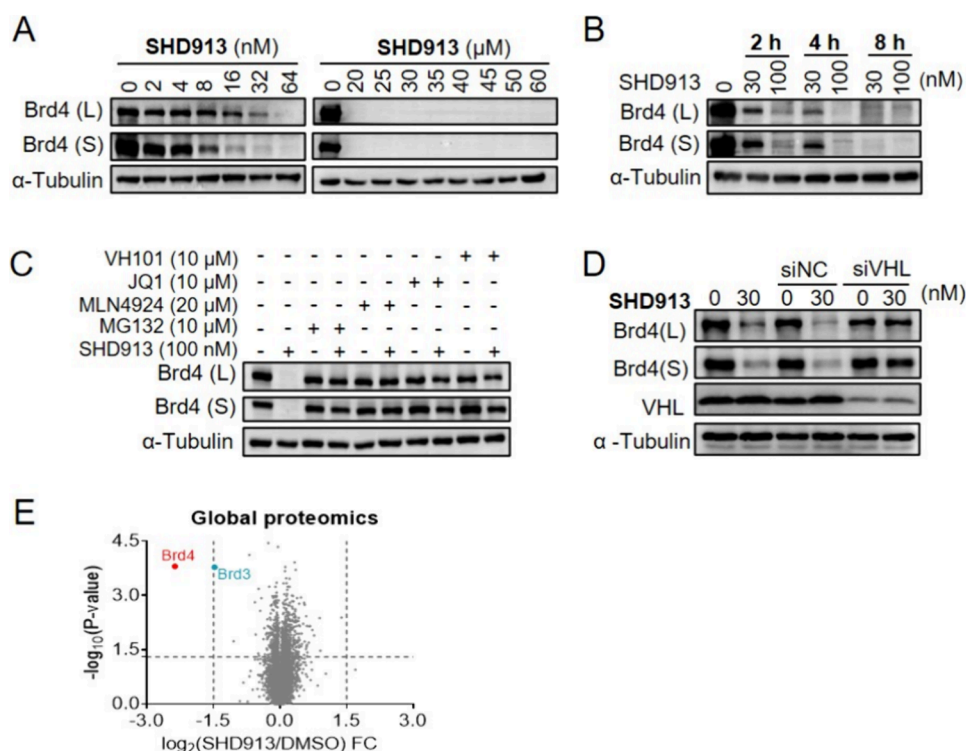
Figure 3. **SHD913** selectively degrades Brd4 via ubiquitin-proteasome degradation mechanism. (A) Immunoblotting analysis of Brd4 in PC-3 cells after treatments of **SHD913** at indicated concentrations for 24 h. (B) Immunoblotting analysis of Brd4 in PC-3 cells after treatment of **SHD913** at 30 or 100 nM for indicated periods of time. (C) Immunoblotting analysis of Brd4 in PC-3 cells pretreated with MG132 (10 μM), MLN-4924 (20 μM), JQ1 (10 μM), or VH101 (10 μM) for 2 h, respectively, followed by treatment with 100 nM of **SHD913** for 2 h. (D) Immunoblotting analysis of Brd4 in PC-3 cells after a 72 h treatment with siRNA-VHL (50 nM) followed by DMSO or 30 nM of SHD913 for 4 h. (E) Proteomic analysis of protein level changes in PC-3 cells after a 2 h treatment with DMSO or 100 nM of **SHD913**.

SHD913, and **10i** are equally potent to **MZ1** under the experimental conditions.

Although the *ortho*-phenyl position of VH032 (8.2 Å) in the Brd4^{BD2}: **MZ1**: VCB complex is slightly farther away from the amide in the JQ1 moiety compared to the benzylic position (7.1 Å), it may also serve as a vector for macrocyclic PROTAC design. Notably, the semiflexible **macroPROTAC-1** was obtained by using this position for cyclization.[12] Therefore, new "Head-to-Tail" macrocyclic PROTACs were also designed and synthesized by using the *ortho*-phenyl position as a docking site, in which longer linker2bs were applied to match the farther distance to the JQ1 amide moiety. The resulting compounds **15a** (*p* = 1), **15b** (*p* = 2), and **15c** (*p* = 3) also demonstrated strong protein degradation on Brd4 at 100 nM, but they were obviously less potent than the benzylicly linked compounds **10d**, **SHD913,** and **10i** at low concentrations (Table 1, Figure S1). Further exploration at this position was hindered by the chemical challenge of the macrocyclization reaction.

Compound SHD913 Selectively Degrades Brd4 through Proteasomal Degradation Process

SHD913 was selected as an example for further biological characterization because of its strong degrading potency and synthetic accessibility. The results showed that **SHD913** potently induced degradation of both the long and short forms of Brd4 in dose- and time-dependent manners in PC3 cells. The compound could obviously degrade the protein at a concentration as low as 2−4 nM, achieving approximately complete degradation (>90%) at 64 nM after 24 h treatment. The DC$_{50}$ values are 7.7 and 5.0 nM for long and short Brd4 isoforms, respectively (Figures 3A and S2A). Moreover, the

compound demonstrated a fast action mode, potently degrading both Brd4 isoforms with rates of 82 and 86%, respectively, after a 2 h exposure at 100 nM (Figure 3B). The ubiquitin-proteasome degradation mechanism was also validated. Pretreatment with either the proteasome inhibitor MG132 or the NEDD8-activating enzyme inhibitor MLN4924 rescued Brd4 from degradation induced by **SHD913** (Figure 3C). BET bromodomain inhibitor JQ1 and VHL ligand VH101 blocked the degradation through binding competition. Additionally, pretreatment with siVHL also reversed SHD913-mediated Brd4 degradation (Figure 3D), supporting a VHL-dependent proteasomal degradation mechanism. Global proteomic analysis was performed by using TMT-labeled mass spectrometry to validate the target specificity of this new macrocyclic PROTAC. Brd4 was the most significantly downregulated protein detected. Although the protein level of Brd3 was also decreased, it was obviously less prominent (Figures 3E and S2B,C). We did not detect Brd2 in the assay, which may be attributed to the low abundance of Brd2 in PC-3 cells.

SHD913 Demonstrates Positive Cooperativity and Dismisses "Hook Effect" in Cancer Cells

"Hook effect" is a common phenomenon and theoretical concern for PROTACs, which results from saturated binary binding of a molecule with either the E3 ligase or the target protein. Strikingly, we did not detect the "hook effect" of **SHD913** even at a super high concentration of 60 μM, which is the maximum applicable concentration and approximately 10,000-fold of the determined DC$_{50}$ value in PC3 cells (Figure 3A). The strong and "linearly" dose-dependent degrading potency of **SHD913** was also validated in other human cancer
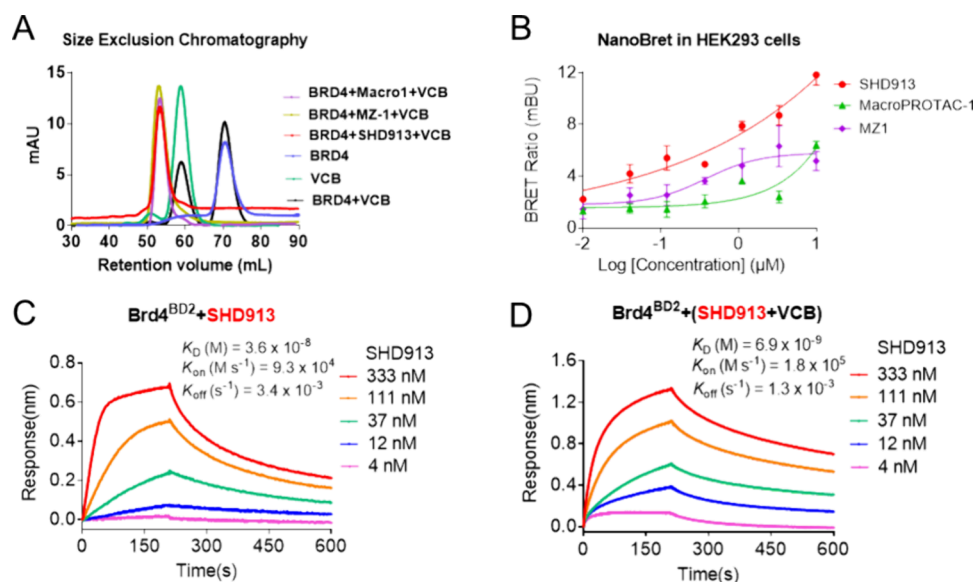
Figure 4. SHD913 induces stable ternary complex formation and demonstrates positive cooperativity. (A) Size-exclusion chromatographic determination of Brd4^{BD2} (blue), VCB (light green), Brd4^{BD2} and VCB (black), and Brd4^{BD2}: **SHD913**(red), **MZ1**(yellow), **macroPROTAC-1**(purple): VCB complex. (B) NanoBRET assay validation of ternary complex formation in HEK293 cells. SHD913(red), **macroPROTAC-1**(green), **MZ1**(purple). (C) **SHD913**: Brd4^{BD2} binary K_d value determination using a biolayer interferometry assay (BLI). Biotinylated Brd4^{BD2} was immobilized on the sensor followed by incubation with different concentrations of **SHD913**. (D) **SHD913**: VCD: Brd4^{BD2} ternary K_d value determination using a BLI assay. Biotinylated Brd4^{BD2} was immobilized on the sensor followed by incubation with designated concentrations of **SHD913** which was preincubated with VCB.

Table 2. Thermodynamic Parameters of Formation of Binary and Ternary Complexes between SHD913, VHL−ElonginC−ElonginB (VCB), and Brd4^{BD2} Measured by Isothermal Titration Calorimetry (ITC) Assay^a

Protein in syringe	Species in cell	K_d [nM]	ΔH [kcal mol^{-1}]	ΔG [kcal mol^{-1}]	$-\Delta TS$ [kcal mo^{l-1}]	α
Brd4^{BD2}	**SHD913**	211.0	−3.46	−9.11	−5.65	
Brd4^{BD2}	**SHD913**: VCB	1.8	−5.75	−11.9	−6.17	117
VCB	**SHD913**	83.4	−4.74	−9.66	−4.92	
VCB	**SHD913**: Brd4^{BD2}	2.3	−5.49	−11.8	−6.29	36

^{a}All ITC titrations were performed at 25 °C. α, cooperativity. Titrations for the binary complex Compound−Brd4^{BD2} or VCB were performed as follows: to the solution of SHD913 (in the cell), protein (38.4 μL) was added by means of a single ITC injection. The ternary complex was titrated followed by the excess solution removed from the cell, the syringe was washed and dried and VCB or Brd4^{BD2} complex was loaded in the syringe and titrated into the diluted PROTAC solution.

cells, including NSCLC cell lines of A549 and NCI-H23, triple negative breast cancer cells MDA-MB-231 and pancreatic cancer cells Panc 10.05 (Figure S2C−F). Whereas, the "hook effect" of **MZ1** was observed starting from 30 μM in PC3 cells, which was consistent with the previous observation (Figure S2G).[21] To confirm that the lack of "hook effect" was not attributed to the solubility or cellular uptake limit of **SHD913**, an intracellular mass detection was conducted to show that the molecule could be dose-dependently accumulated in cells with greater concentrations than those of **MZ-1** and **macro-PROTAC-1** (Figure S2H). These results also promoted us to validate if **SHD913** could induce the formation of a stable ternary complex of Brd4: **SHD913**: VCB. Initially, a size-exclusion chromatography assay was performed, revealing a leftward shift in retention volume upon mixing **SHD913** with purified proteins Brd4^{BD2} and VCB, while no change was observed in the absence of the compound (Figure 4A). This result indicated the formation of a stable ternary complex of Brd4: **SHD913**: VCB. The **SHD913**-induced ternary complex formation in cells was also validated by using a NanoBRET assay. It was shown that **SHD913** dose-dependently induced stronger luminescence signals than **MZ1** and **macroPROTAC-1** in the same experimental setup. It was also noteworthy that **MZ1**

induced a signal saturation at a concentration of 3.3 μM, but the saturation point could not be reached for **SHD913** in this assay, where 10 μM was the highest practicable concentration (Figure 4B). These results collectively suggest that the macrocyclic PROTAC could induce the ternary complex formation more efficiently than the lead compound.

To determine the capability of **SHD913** to induce de novo PPIs, a biolayer interferometry assay (BLI) was first conducted. It was confirmed that there was no intrinsic PPI between Brd4^{BD2} and VCB (Figure S3A). Whereas, preincubating **SHD913** with a concentration gradient of VCB significantly induced interaction between immobilizing biotinylated Brd4^{BD2} and VCB, with a K_d value of 20.0 nM (Figure S3B). The cooperativity factor ($\alpha = K_d^{binary}/K_d^{ternary}$) is a parameter reflecting the capability of a molecule to induce ternary complex formation with two different proteins.[22] Positive cooperativity ($\alpha > 1$) indicates that binding of a molecule with one protein (binary complex) would facilitate and stabilize the formation of a ternary complex with the other one, which is presumably due to favorable chemical-induced PPIs. While negative cooperativity ($\alpha < 1$) suggests that a compound may induce unfavorably steric hindrance between the two proteins, thus a binary complex is detrimental to the formation of a ternary complex.

Noncooperative binding ($\alpha = 1$) means a bivalent molecule is large enough that binding with one protein will not affect its interaction with another one.[23] To evaluate the potential cooperativity of compound **SHD913**, α value was calculated based on the K_d values determined using a BLI assay. The K_d^{binary} and $K_d^{ternary}$ values of **SHD913** with Brd4[BD2] were measured by incubating biotinylated Brd4[BD2] with **SHD913** alone or preincubated with VCB protein, respectively. It was shown that **SHD913** exhibited strong binding to Brd4[BD2] with a K_d^{binary} value of 36.2 nM in the absence of VCB (Figure 4C), while preincubation of **SHD913** with VCB protein significantly favored its Brd4[BD2] binding with a $K_d^{ternary}$ value of 6.9 nM (Figure 4D). Thus, a positive cooperativity for Brd4[BD2] was achieved with an α value of 5.2. The isothermal titration calorimetry (ITC) experiments were also conducted to validate the cooperativity factor of **SHD913**, **MZ1**, and **macro-PROTAC-1**. It was shown that **SHD913** displayed an α value of 117 for Brd4[BD2] in ITC assays (Table 2), which is slightly greater than that of **MZ1** and **macroPROTAC-1** under the same conditions (Figure S4, Table S1). The variation of α values is attributed to the condition difference in the determination assays.[22] These data strongly agreed with the above observation that **SHD913** induced Brd4[BD2]-VHL interaction both in biophysical assays and in cellular NanoBRET determination and significantly mitigated the "hook effect".

Structural Analysis of Brd4[BD2]: SHD913: VCB Ternary Complex

To get structural insight into the **SHD913**-induced ternary complex, a cocrystal structure of Brd4[BD2]: **SHD913**: VCB was solved with a resolution of 2.95 Å (PDB 8YMB, Table S2). Brd4[BD2]: **SHD913**: VCB exhibits quaternary architecture similar to that of Brd4[BD2]: **MZ1**: VCB, and Brd4[BD2]: **macroPROTAC-1**: VCB, with root-mean-square deviation (RMSD) values of 1.092 and 1.079, respectively, through backbone Cα alignment (Figure S5). It is shown that **SHD913** occupies the interface between Brd4[BD2] and VHL with well-defined electron density, serving as a bridge between the proteins to facilitate the formation of a ternary complex (Figures 5A and S6). The JQ1 moiety of **SHD913** binds to the acetyllysine-binding pocket of Brd4[BD2] through a hydrogen bond with N433[Brd4(BD2)] and hydrophobic interaction with WPF shelf, while the VH032 motif attaches to the hydroxyproline-binding site of VHL mediated by multiple hydrogen bonds and stacking interactions (Figure 5B).

These binding patterns closely resemble those observed in previously reported binary crystal structures.[14] Additionally, linker2a in **SHD913** forms hydrophobic interactions with the second helical turn of the ZA loop of Brd4[BD2] and compensates greatly with the cavity formed by interfaces of the two proteins (Figures 5B and S7). Significantly, the optimal linker2a could "drive" the proximity of the two proteins to facilitate PPI formation through conserved bidentate salt bridges between Asp381[Brd4(BD2)], Glu383[Brd4(BD2)], and Arg108[VHL] (Figure 5C). For the three complex structures, a salt bridge between Arg69[VHL] and Glu438[Brd4(BD2)] is only observed in Brd4[BD2]: **MZ1**: VCB. In comparison to the observation of hydrogen-bond mediated by the PEG linker and His437[Brd4(BD2)], as well as hydrogen bonds between Arg107[VHL], His110[VHL], and Ala384[Brd4(BD2)] both in the Brd4[BD2]: **MZ1**: VCB complex and Brd4[BD2]: **macroPROTAC-1**: VCB, there is no defined PPI in the upper part of the Brd4[BD2]: **SHD913**: VCB cocrystal structure (Figure 5C). Subsequently, **SHD913** induced a slightly decreased buried surface area (BSA) of 603 Å² in the
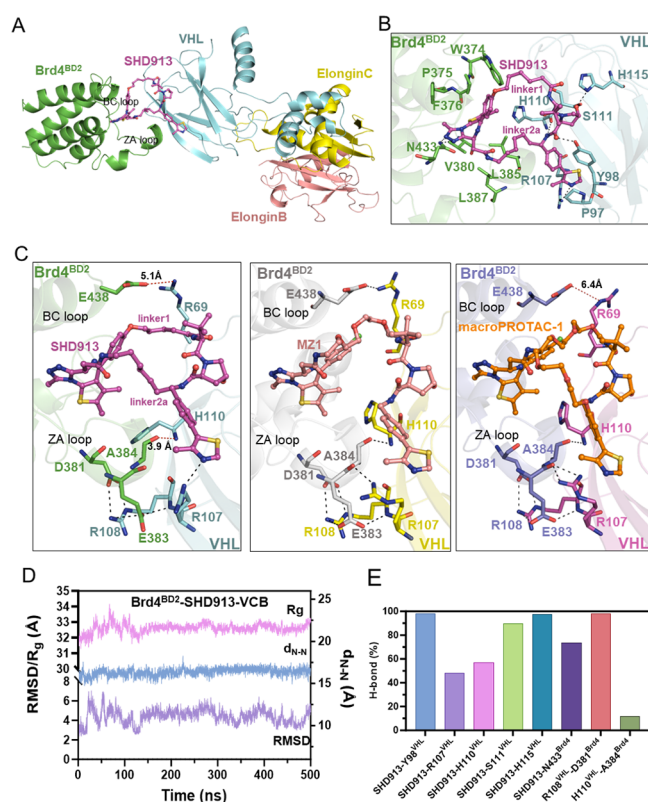

Figure 5. Structure analysis of the ternary complex of Brd4[BD2]: **SHD913**: VCB. (A) Overall structure of ternary complex in cartoon representation (PDB: 8YMB). (B) Close view of binding mode of **SHD913** with Brd4[BD2] and VCB. (C) Comparison of PPIs in Brd4[BD2]: **SHD913**: VCB complex (left) with in Brd4[BD2]: **MZ1**: VCB complex (middle) and Brd4[BD2]: **macroPROTAC-1**: VCB complex (right) through structural analysis. **SHD913** is shown in a stick-and-ball and purple model, while Brd4[BD2] and VHL are shown in green and cyan cartoon, respectively. **MZ1** is shown in a stick-and-ball and salmon model, while Brd4[BD2] and VHL are shown in gray and yellow cartoon, respectively. **MacroPROTAC-1** is shown in a stick-and-ball and orange model. Brd4[BD2] and VHL are shown in slate and purple cartoon, respectively. All sites are shown in the similar orientation after structure superposition of the three structures. Hydrogen bonds and salt bridges are shown as black dashes. Red dashes indicate that the atoms are too far away to contact each other. (D) RMSD of ligand, radius of gyration (Rg) of complex, and dN-O in the 500 ns MD simulations for the Brd4[BD2]: **SHD913**: VCB complex; and (E) hydrogen bond (H-bond) analysis for the Brd4[BD2]: **SHD913**: VCB complex.

protein/protein interface between Brd4[BD2] and VHL, compared to that of **MZ1** (689 Å²) and **macroPROTAC-1** (681 Å²). However, the hydrophobic linker1 in **SHD913** serves as a "hinge" to hijack the two proteins into spatial proximity and compensate for the PPI loss to facilitate and stabilize the ternary complex formation.

Molecular dynamics (MD) simulations were also conducted to explore conformational features of the complex in dynamic settings. Three systems, i.e., Brd4[BD2]: **SHD913**: VCB, Brd4[BD2]: **SHD913**, and **SHD913**: VCB, were prepared from the crystal structure of the ternary complex. Each system was subjected to a 500 ns MD simulation. It was shown that all complexes were stable, as evidenced by minor RMSD fluctuations (Figures 5D and S8A,B). Hydrogen bond analysis of the ternary complex validated the contributions of the hydrogen bond networks, which align with observations from crystal structures. Approximately 95% occupancy was observed for the H-bonds between

the triazole nitrogen of JQ1 and Asn433[Brd4(BD2)], the hydroxyproline of **SHD913** and His110[VHL], and between Arg108[VHL] and Asp381[Brd4(BD2)]. In contrast, the hydrogen bond between His110[VHL] and Ala384[Brd4(BD2)] was notably less significant with only 12% occupancy (Figure 5E). The conformational stability of the macrocyclic PROTAC in binary complexes was also assessed by measuring its RMSD and the distance between the triazole nitrogen and the hydroxyproline (d_{N-O}) (Figure S8A,B). It was shown that **SHD913** adopted substantially stable conformation in both complexes with minor RMSD fluctuations (Figure S8C,D). The d_{N-O} distances were 13.7 ± 0.5 Å in the **SHD913**: Brd4[BD2] complex and 15.1 ± 1.0 Å in the **SHD913**: VCB complex (Figure S8A,B), respectively, which are similar to that observed in the crystal structure (d_{N-O} = 16.0 Å) and ternary complex during MD simulations (d_{N-O} = 16.3 ± 0.4 Å). These data suggested **SHD913** retained a similar conformation in binary complexes as that in ternary complexes, supporting the conformational stability of the macrocyclic PROTAC.

The structural details together with the MD simulation results provide a convincing explanation about the superior efficiency of **SHD913** in inducing ternary complex formation and highlight the advantages of the conformationally restricted macrocyclization approach for new PROTAC design.

CONCLUSIONS

In conclusion, the first "Head-to-Tail" macrocyclic Brd4 PROTAC was designed and synthesized to exemplify the potential application of the macrocyclization strategy in new PROTAC development. The representative macrocyclic molecule **SHD913** exhibited similar degradation potency to that of previously reported linear PROTAC **MZ1**, with low nM DC$_{50}$ values. However, it pronouncedly mitigated the "hook effect", which is a common concern for the PROTAC therapy, in different human cancer cell lines. No measurable "hook effect" was detected at concentrations of approximately 10,000 times greater than the determined DC$_{50}$ values. BLI and ITC biophysical determination supported that the compound exhibited positive cooperativity with α values of 5.2 and 117, respectively. The NanoBRET evaluation also revealed that **SHD913** strongly induced *neomorphic* PPIs between Brd4[BD2] and VHL in cells. The co-crystal structure of Brd4[BD2]: **SHD913**: VCB ternary complex was also determined to elucidate details of the chemical-induced PPIs. MD simulation results validated the crucial contribution of the restricted conformation of **SHD913** to inducing the ternary complex formation. Although further characterization is needed, **SHD913** demonstrates significantly mitigated "hook effect", positive cooperativity, and *de novo* PPI induction. Additionally, preliminary *in vitro* liver microsomal stability of **SHD913** was also evaluated to show that the macrocyclic molecule exhibited improved metabolic stability compared with the linear lead compound in different species (Table S3). These results collectively support the potential advantages of the macrocyclization approach in the new PROTAC design.

METHODS

Chemistry

General Methods for Chemistry. The commercial reagents and solvents were utilized without further purification in chemical synthesis. Reaction progress was monitored using liquid chromatography−mass spectrometry (LC-MS) and thin-layer chromatography (TLC). Intermediates and final compounds underwent purification through column chromatography on silica gel (300−400 mesh) and preparative reversed-phase high-performance liquid chromatography (RP-HPLC, acetonitrile/H$_2$O), respectively. NMR spectra were recorded on a Bruker AVANCE 600 spectrometer (Bruker Company, Germany) in CDCl$_3$, DMSO-d_6, or methanol-d_4. High-resolution mass spectra (HRMS) were obtained using a Bruker MaXis 4G TOF mass spectrometer. The purities of final compounds were assessed via HPLC analysis utilizing the Agilent 1200 system and were confirmed to be >95%. HPLC condition included a Triart C18 reversed-phase column (5 μm, 4.6 mm × 250 mm) with a flow rate of 1.0 mL/min. The gradient started with a 15 min transition from a 0.1% TFA in water and acetonitrile 1:9 mixture to 0.1% TFA in acetonitrile, followed by a 5 min phase of 0.1% TFA in acetonitrile.

(*S*)-2-(4-(4-Hydroxyphenyl)-2,3,9-trimethyl-6*H*-thieno[3,2-*f*][1,2,4]triazolo[4,3-*a*][1,4]diazepin-6-yl)acetic Acid. A solution of (*S*)-2-(4-(4-chlorophenyl)-2,3,9-trimethyl-6*H*-thieno[3,2-*f*][1,2,4]-triazolo[4,3-*a*][1,4]diazepin-6-yl)acetic acid **1** (500 mg, 1.3 mmol, 1.0 equiv), KOH (280 mg, 5.0 mmol, 4.0 equiv), and *t*BuBrettPhos (484 mg, 1.0 mmol, 0.8 equiv) in dioxane/H$_2$O (20 mL, v/v = 4/1) was degassed (argon sparge) before addition of Pd$_2$(dba)$_3$ (220 mg, 0.25 mmol, 0.2 equiv). The resulting mixture was stirred at 100 °C for 12 h under an argon atmosphere before being cooled to RT. Then the mixture was diluted with H$_2$O (20 mL) and extracted with ethyl acetate (EtOAc, 20 mL). The organic phase was separated, and the aqueous phase was washed with EtOAc (10 mL) three times. The resulting aqueous phase was acidified (pH 5−6) with 2 N hydrochloric acid (HCl) and was then concentrated. The obtained residue was redissolved in CH$_2$Cl$_2$/MeOH (20 mL, v/v = 5/1) and was then filtered. The organic phase was concentrated to provide crude intermediate (*S*)-2-(4-(4-hydroxyphenyl)-2,3,9-trimethyl-6*H*-thieno-[3,2-*f*][1,2,4]triazolo[4,3-*a*][1,4]diazepin-6-yl)acetic acid (410 mg, 86%) as a yellow solid, which was used directly without further purification. ¹H NMR (600 MHz, DMSO-d_6) δ 7.25 (d, *J* = 8.1 Hz, 2H), 6.78 (d, *J* = 8.7 Hz, 2H), 4.40 (t, *J* = 6.9 Hz, 1H), 3.20 (dd, *J* = 16.1, 5.8 Hz, 1H), 3.14 (dd, *J* = 16.0, 7.7 Hz, 1H), 2.57 (s, 3H), 2.40 (s, 3H), 1.67 (s, 3H). ¹³C NMR (150 MHz, DMSO-d_6) δ 173.17, 162.78, 160.21, 156.05, 149.23, 131.09, 130.72, 130.24, 130.12, 129.75, 128.26, 115.08, 54.06, 38.29, 13.92, 12.60, 11.09. LC−MS: calcd for C$_{19}$H$_{18}$N$_4$O$_3$S [M + H]⁺ 383.1, found 383.0.

Methyl (*S*)-2-(4-(4-Hydroxyphenyl)-2,3,9-trimethyl-6*H*-thieno[3,2-*f*][1,2,4]triazolo[4,3-*a*][1,4]diazepin-6-yl)acetate (2). To a stirred solution of (*S*)-2-(4-(4-hydroxyphenyl)-2,3,9-trimethyl-6*H*-thieno[3,2-*f*][1,2,4]triazolo[4,3-*a*][1,4]diazepin-6-yl)-acetic acid (382 mg, 1.0 mmol, 1.0 equiv) in MeOH (15 mL) was added thionyl chloride (177 mg, 107 μL, 1.5 mmol, 1.5 equiv) dropwise at 0 °C. The resulting mixture was stirred at RT for 5 h and was then concentrated. The obtained residue was purified by column chromatography (CH$_2$Cl$_2$/MeOH) to give intermediate **2** (376 mg, 95%) as a yellow solid. ¹H NMR (600 MHz, DMSO-d_6) δ 9.92 (s, 1H), 7.25 (d, *J* = 8.3 Hz, 2H), 6.77 (d, *J* = 8.9 Hz, 2H), 4.55−4.16 (m, 1H), 3.66 (s, 3H), 3.45 (dd, *J* = 16.5, 6.7 Hz, 1H), 3.38 (dd, *J* = 16.5, 7.8 Hz, 1H), 2.59 (s, 3H), 2.42 (s, 3H), 1.67 (s, 3H). ¹³C NMR (150 MHz, DMSO-d_6) δ 171.07, 163.50, 159.56, 155.07, 149.65, 131.34, 130.40, 130.33, 130.24, 129.96, 128.64, 114.99, 52.96, 51.42, 36.26, 13.91, 12.61, 11.09. LC−MS: calcd for C$_{20}$H$_{20}$N$_4$O$_3$S [M + H]⁺ 397.1, found 397.1.

***tert*-Butyl (*S*)-5-(4-(6-(2-Methoxy-2-oxoethyl)-2,3,9-trimethyl-6*H*-thieno[3,2-*f*][1,2,4]triazolo[4,3-*a*][1,4]diazepin-4-yl)-phenoxy)pentanoate.** To a stirred suspension of intermediate **2** (350 mg, 0.9 mmol, 1.0 equiv) in acetonitrile (15 mL) was added *tert*-butyl-5-bromopentanoate (320 mg, 1.4 mmol, 1.5 equiv) and K$_2$CO$_3$ (372 mg, 2.7 mmol, 3.0 equiv). The reaction mixture was heated to 80 °C for 12 h and was then cooled to RT. The slurry was filtered, and the resulting cake was washed with EtOAc (10 mL). The organic phase was concentrated, and the resulting residue was then purified by column chromatography (CH$_2$Cl$_2$/MeOH) to give intermediate *tert*-butyl (*S*)-5-(4-(6-(2-methoxy-2-oxoethyl)-2,3,9-trimethyl-6*H*-thieno[3,2-*f*]-[1,2,4]triazolo[4,3-*a*][1,4]diazepin-4-yl)phenoxy)pentanoate (432 mg, 87%) as a white solid. ¹H NMR (600 MHz, DMSO-d_6) δ 7.34 (d, *J* = 8.4 Hz, 2H), 6.94 (d, *J* = 8.9 Hz, 2H), 4.44 (t, *J* = 7.2 Hz, 1H),

3.99 (t, J = 6.3 Hz, 2H), 3.66 (s, 3H), 3.46 (dd, J = 16.5, 6.7 Hz, 1H), 3.39 (dd, J = 16.5, 7.8 Hz, 1H), 2.60 (s, 3H), 2.42 (s, 3H), 2.25 (t, J = 7.3 Hz, 2H), 1.75−1.68 (m, 2H), 1.65 (s, 3H), 1.64−1.59 (m, 2H), 1.39 (s, 9H). ^{13}C NMR (150 MHz, DMSO-d_6) δ 172.60, 171.63, 163.99, 160.93, 155.53, 150.30, 132.15, 131.04, 130.70, 130.66, 130.45, 114.62, 79.95, 67.71, 53.63, 52.01, 36.82, 34.86, 28.39, 28.23, 21.74, 14.51, 13.18, 11.69. LC-MS: calcd for $C_{29}H_{36}N_4O_5S$ [M + H]$^+$ 553.2, found 553.3.

(S)-2-(4-(4-((5-(tert-Butoxy)-5-oxopentyl)oxy)phenyl)-2,3,9-trimethyl-6H-thieno[3,2-f][1,2,4]triazolo[4,3-a][1,4]diazepin-6-yl)acetic Acid (4b). To a solution of *tert*-butyl (*S*)-5-(4-(6-(2-methoxy-2-oxoethyl)-2,3,9-trimethyl-6*H*-thieno[3,2-*f*][1,2,4]triazolo-[4,3-*a*][1,4]diazepin-4-yl)phenoxy)pentanoate (400 mg, 0.7 mmol, 1.0 equiv) in THF/H$_2$O (15 mL, v/v = 2/1) was added LiOH (52 mg, 2.1 mmol, 3.0 equiv). The reaction mixture was stirred at RT for 4 h before being concentrated to remove THF. The resulting aqueous phase was acidified (pH 5−6) with 2 N HCl before being extracted with EtOAc (30 mL). The organic phase was dried with anhydrous sodium sulfate (Na$_2$SO$_4$), filtered, and concentrated to yield a light yellow solid, which was resuspended via a mixture solution of isopropyl acetate and petroleum ether (PE) and was then filtered to give intermediate **4b** (362 mg, 93%) as a white solid. ^{1}H NMR (600 MHz, DMSO-d_6) δ 12.37 (brs, 1H), 7.36 (d, J = 8.4 Hz, 2H), 6.95 (d, J = 9.1 Hz, 2H), 4.40 (t, J = 7.1 Hz, 1H), 3.99 (t, J = 6.3 Hz, 2H), 3.41 (dd, J = 16.6, 6.9 Hz, 1H), 3.29 (dd, J = 16.6, 7.4 Hz, 1H), 2.60 (s, 3H), 2.42 (s, 3H), 2.26 (t, J = 7.3 Hz, 2H), 1.75−1.68 (m, 2H), 1.66 (s, 3H), 1.66−1.58 (m, 3H), 1.39 (s, 9H). ^{13}C NMR (150 MHz, DMSO-d_6) δ 171.51, 171.50, 162.72, 159.82, 154.66, 149.12, 131.01, 129.92, 129.66, 129.61, 129.59, 129.34, 113.53, 78.86, 66.62, 52.70, 36.04, 33.77, 27.31, 27.15, 27.13, 20.65, 13.44, 12.09, 10.61. LC-MS: calcd for $C_{28}H_{34}N_4O_5S$ [M + H]$^+$ 539.2, found 539.2.

(S)-2-(4-(4-(4-(tert-Butoxy)-4-oxobutoxy)phenyl)-2,3,9-tri-methyl-6H-thieno[3,2-f][1,2,4]triazolo[4,3-a][1,4]diazepin-6-yl)acetic Acid (4a). Intermediate **4a** was prepared via a similar procedure to that of compound **4b**. ^{1}H NMR (600 MHz, DMSO-d_6) δ 12.41 (brs, 1H), 7.37 (d, J = 8.2 Hz, 2H), 6.95 (d, J = 8.9 Hz, 2H), 4.41 (t, J = 7.1 Hz, 1H), 4.00 (t, J = 6.3 Hz, 2H), 3.41 (dd, J = 16.6, 6.9 Hz, 1H), 3.30 (dd, J = 16.6, 7.4 Hz, 1H), 2.60 (s, 3H), 2.42 (s, 3H), 2.36 (t, J = 7.3 Hz, 2H), 1.93 (p, J = 6.8 Hz, 2H), 1.66 (s, 3H), 1.39 (s, 9H). ^{13}C NMR (150 MHz, DMSO-d_6) δ 172.54, 172.30, 163.93, 160.90, 155.70, 150.26, 132.23, 131.08, 130.70, 130.64, 130.53, 114.63, 80.17, 67.16, 53.72, 37.04, 31.74, 28.23, 24.73, 14.52, 13.18, 11.70. LC-MS: calcd for $C_{27}H_{32}N_4O_5S$ [M + H]$^+$ 525.2, found 525.0.

(S)-2-(4-(4-(6-(tert-Butoxy)-6-oxohexyl)oxy)phenyl)-2,3,9-trimethyl-6H-thieno[3,2-f][1,2,4]triazolo[4,3-a][1,4]diazepin-6-yl)acetic Acid (4c). Intermediate **4c** was prepared via a similar procedure to that of compound **4b**. ^{1}H NMR (600 MHz, DMSO-d_6) δ 12.41 (brs, 1H), 7.36 (d, J = 8.3 Hz, 2H), 6.94 (d, J = 9.0 Hz, 2H), 4.40 (t, J = 7.1 Hz, 1H), 3.98 (t, J = 6.4 Hz, 2H), 3.41 (dd, J = 16.6, 6.9 Hz, 1H), 3.30 (dd, J = 16.6, 7.4 Hz, 1H), 2.60 (s, 3H), 2.42 (s, 3H), 2.20 (t, J = 7.2 Hz, 2H), 1.75−1.68 (m, 2H), 1.66 (s, 3H), 1.58−1.50 (m, 2H), 1.43−1.36 (m, 11H). ^{13}C NMR (150 MHz, DMSO-d_6) δ 172.68, 172.56, 163.88, 161.01, 155.73, 150.23, 132.16, 131.04, 130.70, 130.57, 130.47, 114.61, 79.86, 67.92, 53.74, 37.08, 35.17, 28.73, 28.23, 25.41, 24.83, 14.52, 13.18, 11.70. LC-MS: calcd for $C_{29}H_{36}N_4O_5S$ [M + H]$^+$ 553.2, found 553.2.

(S)-2-(4-(4-((7-(tert-Butoxy)-7-oxoheptyl)oxy)phenyl)-2,3,9-trimethyl-6H-thieno[3,2-f][1,2,4]triazolo[4,3-a][1,4]diazepin-6-yl)acetic Acid (4d). Intermediate **4d** was prepared via a similar procedure to that of compound **4b**. ^{1}H NMR (600 MHz, DMSO-d_6) δ 7.35 (d, J = 8.4 Hz, 2H), 6.94 (d, J = 9.0 Hz, 2H), 4.40 (t, J = 7.1 Hz, 1H), 3.97 (t, J = 6.4 Hz, 2H), 3.39 (dd, J = 16.6, 6.9 Hz, 1H), 3.26 (dd, J = 16.6, 7.3 Hz, 1H), 2.59 (s, 3H), 2.42 (s, 3H), 2.18 (t, J = 7.3 Hz, 2H), 1.73−1.67 (m, 2H), 1.66 (s, 3H), 1.53−1.47 (m, 2H), 1.43−1.35 (m, 11H), 1.34−1.27 (m, 2H). ^{13}C NMR (150 MHz, DMSO-d_6) δ 171.65, 162.61, 159.87, 154.79, 149.05, 130.98, 129.89, 129.70, 129.58, 129.32, 113.50, 78.73, 66.89, 52.86, 34.05, 27.80, 27.49, 27.14, 24.52, 23.90, 13.43, 12.09, 10.60. LC-MS: calcd for $C_{30}H_{38}N_4O_5S$ [M + H]$^+$ 567.3, found 567.5.

tert-Butyl (S)-(4-Azido-1-(4-(4-methylthiazol-5-yl)phenyl)-butyl)carbamate (6a). To a stirred solution of compound **5a** (360

mg, 1.0 mmol, 1.0 equiv) in anhydrous DMF/Toluene (20 mL, v/v = 1/10) was added DBU (380 mg, 348 μL, 2.5 mmol, 2.5 equiv) and DPPA (687 mg, 2.5 mmol, 2.5 equiv). The mixture was stirred at 50 °C for 12 h before being diluted with H$_2$O (30 mL). The resulting solution was extracted with EtOAc (30 mL). The organic phase was dried with anhydrous Na$_2$SO$_4$, filtered, and concentrated to afford a colorless oil, which was then purified by column chromatography (PE/EtOAc) to yield intermediate **6a** (340 mg, 88%) as a colorless oil. ^{1}H NMR (600 MHz, Methanol-d_4) δ 8.86 (s, 1H), 7.44 (d, J = 8.2 Hz, 2H), 7.40 (d, J = 8.2 Hz, 2H), 4.60 (t, J = 7.1 Hz, 1H), 3.36−3.31 (m, 2H), 2.48 (s, 3H), 1.80 (q, J = 7.3 Hz, 2H), 1.74−1.65 (m, 1H), 1.63−1.54 (m, 1H), 1.43 (s, 9H). ^{13}C NMR (150 MHz, Methanol-d_4) δ 157.96, 152.85, 149.11, 145.31, 133.43, 131.57, 130.46, 128.00, 80.29, 55.45, 52.14, 34.95, 28.81, 27.09, 15.85. LC-MS: calcd for $C_{19}H_{25}N_5O_2S$ [M + H]$^+$ 388.2, found 388.2. Intermediates **6b−6f** were prepared via a similar procedure to that of compound **6a**.

tert-Butyl ((S)-1-((2S,4R)-2-(((S)-4-Azido-1-(4-(4-methylthia-zol-5-yl)phenyl)butyl)carbamoyl)-4-hydroxypyrrolidin-1-yl)-3,3-dimethyl-1-oxobutan-2-yl)carbamate. To a solution of compound **6a** (320 mg, 0.8 mmol, 1.0 equiv) in CH$_2$Cl$_2$ (15 mL) was added TFA (3 mL) before being stirred at RT for 3 h. The reaction solution was concentrated to remove TFA and obtain a yellow oil, which was dissolved in DMF (15 mL). Commercial (2S,4R)-1-((S)-2-((*tert*-butoxycarbonyl)amino)-3,3-dimethylbutanoyl)-4-hydroxypyrro-lidine-2-carboxylic acid **7** (310 mg, 0.9 mmol, 1.1 equiv), Et$_3$N (414 mg, 520 μL, 4.1 mmol, 5.0 equiv), and HATU (405 mg, 1.0 mmol, 1.3 equiv) were then added. The resulting mixture was stirred at RT for 5 h, then diluted with H$_2$O (50 mL) and extracted with EtOAc (40 mL). The resulting organic phase was washed with saline water, dried, filtered, and concentrated to give a colorless oil, which was purified by column chromatography (MeOH/CH$_2$Cl$_2$) to obtain intermediate *tert*-butyl ((S)-1-((2S,4R)-2-(((S)-4-azido-1-(4-(4-methylthiazol-5-yl)-phenyl)butyl)carbamoyl)-4-hydroxypyrrolidin-1-yl)-3,3-dimethyl-1-oxobutan-2-yl)carbamate (306 mg, 61% over two steps) as a colorless oil. ^{1}H NMR (600 MHz, DMSO-d_6) δ 8.99 (s, 1H), 8.49 (d, J = 8.5 Hz, 1H), 7.45 (d, J = 8.3 Hz, 2H), 7.39 (d, J = 8.3 Hz, 2H), 6.37 (d, J = 9.2 Hz, 1H), 5.11 (d, J = 3.1 Hz, 1H), 4.87 (q, J = 7.5 Hz, 1H), 4.46 (t, J = 8.0 Hz, 1H), 4.31 (s, 1H), 4.14 (d, J = 9.3 Hz, 1H), 3.62 (dd, J = 10.5, 3.9 Hz, 1H), 3.58 (d, J = 10.3 Hz, 1H), 3.37−3.33 (m, 2H), 2.46 (s, 3H), 2.02−1.94 (m, 1H), 1.82−1.67 (m, 4H), 1.65−1.58 (m, 1H), 1.39 (s, 9H), 0.94 (s, 9H). ^{13}C NMR (150 MHz, DMSO-d_6) δ 171.54, 170.16, 155.78, 151.98, 148.28, 143.98, 131.54, 130.33, 129.33, 127.26, 78.54, 69.33, 59.13, 58.85, 56.79, 51.68, 50.87, 38.19, 35.87, 33.94, 28.65, 26.75, 26.72, 25.62, 16.48. LC-MS: calcd for $C_{30}H_{43}N_7O_5S$ [M + H]$^+$ 614.3, found 614.2.

tert-Butyl ((S)-1-((2S,4R)-2-(((S)-4-Amino-1-(4-(4-methylthia-zol-5-yl)phenyl)butyl)carbamoyl)-4-hydroxypyrrolidin-1-yl)-3,3-dimethyl-1-oxobutan-2-yl)carbamate (8a). To a solution of intermediate *tert*-butyl ((S)-1-((2S,4R)-2-(((S)-4-azido-1-(4-(4-meth-ylthiazol-5-yl)phenyl)butyl)carbamoyl)-4-hydroxypyrrolidin-1-yl)-3,3-dimethyl-1-oxobutan-2-yl)carbamate (280 mg, 0.5 mmol, 1.0 equiv) in 1,4-dioxane/H$_2$O (20 mL, v/v = 5/1) was added triphenylphosphine (360 mg, 1.4 mmol, 3.0 equiv). The mixture was stirred at RT for 1 h. Further NH$_3$·H$_2$O (2 mL) was then added. The resulting solution was stirred at RT for another 11 h before being concentrated. The residue was purified by column chromatography (0.5% Et$_3$N in MeOH/CH$_2$Cl$_2$) to obtain intermediate **8a** (247 mg, 92%) as a white solid. ^{1}H NMR (600 MHz, DMSO-d_6) δ 8.99 (s, 1H), 8.49 (d, J = 8.4 Hz, 1H), 7.44 (d, J = 8.3 Hz, 2H), 7.39 (d, J = 8.3 Hz, 2H), 6.51 (d, J = 9.3 Hz, 1H), 5.15 (brs, 1H), 4.82 (td, J = 8.9, 5.7 Hz, 1H), 4.46 (t, J = 8.0 Hz, 1H), 4.30 (s, 1H), 4.16 (d, J = 9.4 Hz, 1H), 3.61 (dd, J = 10.5, 3.9 Hz, 1H), 3.57 (d, J = 10.3 Hz, 1H), 2.68−2.58 (m, 2H), 2.46 (s, 3H), 2.03−1.98 (m, 1H), 1.79−1.65 (m, 3H), 1.59−1.47 (m, 2H), 1.40−1.37 (m, 10H), 1.28−1.22 (m, 1H), 0.93 (s, 9H). ^{13}C NMR (150 MHz, DMSO-d_6)) δ 170.81, 169.62, 155.22, 151.38, 147.65, 143.73, 131.00, 129.62, 128.68, 126.72, 77.98, 68.70, 58.58, 58.27, 56.29, 51.36, 40.14, 37.63, 35.36, 33.29, 28.10, 27.56, 26.22, 15.91. LC-MS: calcd for $C_{30}H_{45}N_5O_5S$ [M + H]$^+$ 588.3, found 588.3.

tert-Butyl ((S)-1-((2S,4R)-2-(((S)-5-Amino-1-(4-(4-methylthia-zol-5-yl)phenyl)pentyl)carbamoyl)-4-hydroxypyrrolidin-1-yl)-

3,3-dimethyl-1-oxobutan-2-yl)carbamate (8b). Intermediate **8b** was prepared via a similar procedure to that of compound **8a**. ^{1}H NMR (600 MHz, DMSO-d_6) δ 8.98 (s, 1H), 8.41 (d, J = 8.4 Hz, 1H), 7.43 (d, J = 8.3 Hz, 1H), 7.37 (d, J = 8.3 Hz, 2H), 6.40 (d, J = 9.3 Hz, 1H), 5.12 (brs, 1H), 4.80 (td, J = 8.7, 5.6 Hz, 1H), 4.47 (t, J = 8.0 Hz, 1H), 4.29 (s, 1H), 4.14 (d, J = 9.4 Hz, 1H), 3.61 (dd, J = 10.5, 4.1 Hz, 1H), 3.56 (d, J = 10.6 Hz, 1H), 2.46 (s, 3H), 2.03−1.94 (m, 1H), 1.79−1.72 (m, 1H), 1.72−1.59 (m, 2H), 1.50−1.17 (m, 17H), 0.93 (s, 9H). ^{13}C NMR (150 MHz, DMSO-d_6) δ 170.79, 169.57, 155.22, 151.36, 147.64, 143.87, 131.01, 129.57, 128.67, 126.69, 77.99, 68.71, 58.49, 58.29, 56.20, 51.85, 41.03, 37.62, 36.18, 35.29, 32.09, 28.09, 26.24, 26.20, 22.91, 15.92. LC-MS: calcd for $C_{31}H_{47}N_5O_5S$ [M + H]$^+$ 602.3, found 602.2.

tert-Butyl ((*S*)-1-((2*S*,4*R*)-2-(((*S*)-6-Amino-1-(4-(4-methylthiazol-5-yl)phenyl)hexyl)carbamoyl)-4-hydroxypyrrolidin-1-yl)-3,3-dimethyl-1-oxobutan-2-yl)carbamate (8c). Intermediate **8c** was prepared via a similar procedure to that of compound **8a**. ^{1}H NMR (600 MHz, DMSO-d_6) δ 8.99 (s, 1H), 8.42 (d, J = 8.2 Hz, 1H), 7.43 (d, J = 8.3 Hz, 2H), 7.37 (d, J = 8.2 Hz, 2H), 6.39 (d, J = 9.1 Hz, 1H), 5.13 (brs, 1H), 4.80 (td, J = 8.7, 6.1 Hz, 1H), 4.46 (t, J = 8.0 Hz, 1H), 4.29 (s, 1H), 4.15 (d, J = 9.2 Hz, 1H), 3.60 (dd, J = 10.5, 4.0 Hz, 1H), 3.56 (d, J = 9.8 Hz, 1H), 2.72−2.67 (m, 2H), 2.46 (s, 3H), 2.06−1.95 (m, 1H), 1.77−1.60 (m, 3H), 1.50−1.20 (m, 22H), 0.93 (s, 9H). ^{13}C NMR (150 MHz, DMSO-d_6) δ 171.36, 170.13, 155.79, 151.97, 148.23, 144.45, 131.57, 130.17, 129.26, 127.24, 78.61, 69.26, 59.03, 58.85, 56.81, 52.24, 38.22, 36.67, 35.87, 28.99, 28.95, 28.67, 26.81, 26.78, 26.05, 16.50. LC-MS: calcd for $C_{32}H_{49}N_5O_5S$ [M + H]$^+$ 616.4, found 616.3.

tert-Butyl ((*S*)-1-((2*S*,4*R*)-2-(((*S*)-7-Amino-1-(4-(4-methylthiazol-5-yl)phenyl)heptyl)carbamoyl)-4-hydroxypyrrolidin-1-yl)-3,3-dimethyl-1-oxobutan-2-yl)carbamate (8d). Intermediate **8d** was prepared via a similar procedure to that of compound **8a**. ^{1}H NMR (600 MHz, DMSO-d_6) δ 8.98 (s, 1H), 8.38 (d, J = 8.4 Hz, 1H), 7.43 (d, J = 8.3 Hz, 2H), 7.36 (d, J = 8.3 Hz, 2H), 6.45 (d, J = 9.4 Hz, 1H), 5.11 (brs, 1H), 4.79 (td, J = 8.7, 5.5 Hz, 1H), 4.46 (t, J = 8.0 Hz, 1H), 4.29 (s, 1H), 4.13 (d, J = 9.3 Hz, 1H), 3.64−3.59 (m, 1H), 3.55 (d, J = 10.6 Hz, 1H), 2.46 (s, 3H), 2.03−1.94 (m, 1H), 1.78−1.70 (m, 1H), 1.71−1.58 (m, 2H), 1.46−1.17 (m, 18H), 0.93 (s, 9H). ^{13}C NMR (150 MHz, DMSO-d_6) δ 170.78, 169.53, 155.23, 151.37, 147.63, 143.89, 131.00, 129.56, 128.66, 126.68, 77.95, 68.69, 58.45, 58.29, 56.13, 51.81, 40.88, 37.60, 36.30, 35.24, 31.64, 28.47, 28.08, 28.04, 26.20, 26.07, 25.48, 15.91. LC-MS: calcd for $C_{33}H_{51}N_5O_5S$ [M + H]$^+$ 630.4, found 630.2.

tert-Butyl ((*S*)-1-((2*S*,4*R*)-2-(((*S*)-8-Amino-1-(4-(4-methylthiazol-5-yl)phenyl)octyl)carbamoyl)-4-hydroxypyrrolidin-1-yl)-3,3-dimethyl-1-oxobutan-2-yl)carbamate (8e). Intermediate **8e** was prepared via a similar procedure to that of compound **8a**. ^{1}H NMR (600 MHz, DMSO-d_6) δ 8.98 (s, 1H), 8.38 (d, J = 8.2 Hz, 1H), 7.43 (d, J = 8.2 Hz, 2H), 7.37 (d, J = 8.2 Hz, 2H), 6.43 (d, J = 9.1 Hz, 1H), 4.79 (td, J = 8.7, 6.0 Hz, 1H), 4.47 (t, J = 7.8 Hz, 1H), 4.29 (s, 1H), 4.14 (d, J = 9.2 Hz, 1H), 3.61 (dd, J = 10.5, 4.0 Hz, 1H), 3.56 (d, J = 10.1 Hz, 1H), 2.46 (s, 3H), 2.01−1.96 (m, 1H), 1.79−1.73 (m, 1H), 1.71−1.59 (m, 2H), 1.45−1.20 (m, 22H), 0.93 (s, 9H). ^{13}C NMR (150 MHz, DMSO-d_6) δ 170.28, 169.02, 154.71, 150.85, 147.12, 143.38, 130.50, 129.04, 128.15, 126.18, 77.44, 68.18, 57.93, 57.77, 55.62, 51.31, 40.54, 37.09, 35.87, 34.74, 31.58, 28.22, 28.17, 27.56, 27.52, 25.71, 25.68, 24.97, 15.39. LC-MS: calcd for $C_{34}H_{53}N_5O_5S$ [M + H]$^+$ 644.4, found 644.3.

tert-Butyl ((*S*)-1-((2*S*,4*R*)-2-(((*S*)-9-Amino-1-(4-(4-methylthiazol-5-yl)phenyl)nonyl)carbamoyl)-4-hydroxypyrrolidin-1-yl)-3,3-dimethyl-1-oxobutan-2-yl)carbamate (8f). Intermediate **8f** was prepared via a similar procedure to that of compound **8a**. ^{1}H NMR (600 MHz, DMSO-d_6) δ 8.98 (s, 1H), 8.38 (d, J = 8.4 Hz, 1H), 7.43 (d, J = 8.3 Hz, 2H), 7.36 (d, J = 8.3 Hz, 2H), 6.41 (d, J = 9.3 Hz, 1H), 4.78 (dt, J = 8.7, 4.4 Hz, 1H), 4.47 (t, J = 7.9 Hz, 1H), 4.29 (s, 1H), 4.14 (d, J = 9.2 Hz, 1H), 3.61 (dd, J = 10.5, 4.1 Hz, 1H), 3.56 (d, J = 10.4 Hz, 1H), 2.46 (s, 3H), 2.02−1.94 (m, 1H), 1.78−1.72 (m, 1H), 1.72−1.58 (m, 2H), 1.40−1.35 (m, 13H), 1.29−1.23 (m, 11H), 0.93 (s, 9H). ^{13}C NMR (150 MHz, DMSO-d_6) δ 170.78, 169.53, 155.22, 151.36, 147.64, 143.89, 131.01, 129.56, 128.66, 126.69, 77.96, 68.70, 58.44, 58.28, 56.14, 51.82, 40.91, 37.61, 36.36, 35.24, 31.83, 28.83, 28.79, 28.64, 28.08, 28.03, 26.24, 26.20, 26.19, 26.14, 25.52, 15.91. LC-MS: calcd for $C_{35}H_{55}N_5O_5S$ [M + H]$^+$ 659.4, found 659.1.

tert-Butyl 5-(4-((*S*)-6-(2-(((*S*)-4-((2*S*,4*R*)-1-((*S*)-2-((*tert*-Butoxycarbonyl)amino)-3,3-dimethylbutanoyl)-4-hydroxy-pyrrolidine-2-carboxamido)-4-(4-(4-methylthiazol-5-yl)-phenyl)butyl)amino)-2-oxoethyl)-2,3,9-trimethyl-6*H*-thieno-[3,2-*f*][1,2,4]triazolo[4,3-*a*][1,4]diazepin-4-yl)phenoxy)-pentanoate (9a). To a solution of intermediate **4b** (80 mg, 0.15 mmol, 1.0 equiv) in DMF (10 mL) was added **8a** (87 mg, 0.15 mmol, 1.0 equiv), Et$_3$N (45 mg, 56 μL, 0.45 mmol, 3.0 equiv), and HATU (73 mg, 0.20 mmol, 1.3 equiv). The reaction mixture was stirred at RT for 5 h before being diluted with H$_2$O (20 mL) and extracted with EtOAc (20 mL). The resulting organic phase was washed with saline water, dried, filtered, and concentrated to obtain a residue, which was purified by column chromatography (MeOH/CH$_2$Cl$_2$) to obtain intermediate **9a** (93 mg, 57%) as a white solid. ^{1}H NMR (600 MHz, Methanol-d_4) δ 8.87 (s, 1H), 7.47−7.39 (m, 4H), 7.34 (d, J = 8.3 Hz, 2H), 6.84 (d, J = 8.9 Hz, 2H), 5.02 (dd, J = 9.9, 4.8 Hz, 1H), 4.63 (dd, J = 9.2, 7.6 Hz, 1H), 4.58 (dd, J = 9.1, 5.2 Hz, 1H), 4.46 (s, 1H), 4.29 (s, 1H), 3.95 (t, J = 6.0 Hz, 2H), 3.87 (d, J = 11.1 Hz, 1H), 3.77 (dd, J = 11.0, 3.9 Hz, 1H), 3.47−3.38 (m, 2H), 3.29−3.19 (m, 2H), 2.68 (s, 3H), 2.46 (s, 3H), 2.42 (s, 3H), 2.27 (t, J = 7.1 Hz, 2H), 2.18 (dd, J = 13.1, 7.6 Hz, 1H), 2.00−1.93 (m, 2H), 1.89−1.86 (m, 1H), 1.83−1.67 (m, 6H), 1.65 (s, 3H), 1.43 (s, 9H), 1.36 (s, 9H), 1.04 (s, 9H). ^{13}C NMR (150 MHz, Methanol-d_4) δ 174.76, 173.82, 172.90, 172.82, 166.95, 162.81, 157.86, 157.42, 152.92, 152.05, 149.13, 144.65, 133.38, 133.06, 132.95, 132.76, 132.52, 131.72, 131.62, 131.49, 130.52, 128.19, 115.41, 81.50, 80.59, 71.16, 68.80, 60.88, 60.40, 58.12, 55.04, 53.75, 39.89, 39.05, 38.82, 36.95, 36.05, 34.67, 29.66, 28.68, 28.40, 27.26, 27.04, 22.89, 15.96, 14.44, 12.96, 11.61. LC-MS: calcd for $C_{58}H_{77}N_9O_9S_2$ [M + H]$^+$ 1108.5, found 1108.8. Intermediates **9b−i** were prepared via a similar procedure to that of compound **9a**.

(1^6*S*,12^2*S*,12^4*R*,10*S*,15*S*,*Z*)-10-(*tert*-Butyl)-12^4-hydroxy-1,2^1,3^{1}9-trimethyl-15-(4-(4-methylthiazol-5-yl)phenyl)-1^6*H*-3-oxa-9,14,19-triaza-1(4,6)-thieno[3,2-*f*][1,2,4]triazolo[4,3-*a*]-[1,4]diazepina-12(1,2)-pyrrolidina-2(1,4)-benzenacycloheni-cosaphane-8,11,13,20-tetraone (10a). To a solution of intermediate **9a** (80 mg, 0.07 mmol, 1.0 equiv) in CH$_2$Cl$_2$ (10 mL) was added TFA (2.5 mL). The resulting solution was stirred at RT for 3 h before being concentrated to obtain a yellow oil, which was dissolved in DMF (30 mL, 0.0025 mM). DIEA (46 mg, 63 μL, 0.36 mmol, 5.0 equiv) and HATU (36 mg, 0.09 mmol, 1.3 equiv) were then added. The resulting mixture was stirred at RT for another 5 h before being concentrated. The resulting residue was purified by preparative reversed-phase high-performance liquid chromatography (RP-HPLC, acetonitrile/H$_2$O) to obtain final compound **10a** (35 mg, 52% over two steps) as a *trans* isomer, white solid. ^{1}H NMR (600 MHz, Methanol-d_4) δ 8.87 (s, 1H), 7.53−7.42 (m, 4H), 7.41 (d, J = 8.3 Hz, 1H), 7.17 (d, J = 8.5 Hz, 1H), 4.84−4.81 (m, 1H), 4.77 (s, 1H), 4.70−4.64 (m, 1H), 4.61 (dd, J = 11.6, 2.3 Hz, 1H), 4.38 (s, 1H), 4.10−4.04 (m, 1H), 4.04−3.99 (m, 1H), 3.84 (d, J = 11.2 Hz, 1H), 3.71 (dd, J = 11.1, 3.8 Hz, 1H), 3.69−3.64 (m, 1H), 3.51 (dd, J = 14.4, 11.6 Hz, 1H), 3.04 (dd, J = 14.3, 2.4 Hz, 1H), 2.98−2.89 (m, 1H), 2.70 (s, 3H), 2.48 (s, 3H), 2.45 (s, 3H), 2.45−2.40 (m, 1H), 2.37−2.30 (m, 1H), 2.25−2.19 (m, 1H), 2.00−1.82 (m, 5H), 1.82−1.75 (m, 3H), 1.74 (s, 3H), 1.72−1.64 (m, 1H), 1.04 (s, 9H). ^{13}C NMR (150 MHz, Methanol-d_4) δ 175.33, 173.94, 173.02, 171.74, 166.57, 162.72, 157.61, 152.91, 152.14, 149.11, 145.65, 133.42, 133.03, 133.00, 132.83, 132.44, 131.96, 131.59, 131.48, 130.51 (2C), 127.94 (2C), 115.99, 70.92, 69.55, 60.34, 58.67, 58.14, 55.80, 54.79, 49.61, 40.77, 39.06, 38.87, 37.06 (2C), 35.52, 35.26, 28.50, 27.64 (3C), 27.13, 24.48, 15.85, 14.53, 12.99, 11.62. HRMS (ESI) calcd for $C_{49}H_{59}N_9O_6S_2$ [M + H]$^+$ 934.4105, found 934.4104. HPLC purity 97.46%. $[\alpha]_D^{25}$ = +4.6 (c = 1.0 mg/mL, acetone).

(1^6*S*,12^2*S*,12^4*R*,10*S*,15*S*,*Z*)-10-(*tert*-Butyl)-12^4-hydroxy-1,2^1,3^{1}9-trimethyl-15-(4-(4-methylthiazol-5-yl)phenyl)-1^6*H*-3-oxa-9,14,20-triaza-1(4,6)-thieno[3,2-*f*][1,2,4]triazolo[4,3-*a*]-[1,4]diazepina-12(1,2)-pyrrolidina-2(1,4)-benzenacyclodoco-saphane-8,11,13,21-tetraone (10b). Final compound **10b** was prepared via a similar procedure to that of compound **10a** as a *trans* isomer, white solid. ^{1}H NMR (600 MHz, Methanol-d_4) δ 8.87 (s, 1H), 7.47−7.40 (m, 6H), 7.15 (d, J = 8.9 Hz, 2H), 4.92 (t, J = 7.5 Hz, 1H), 4.70 (s, 1H), 4.61−4.53 (m, 2H), 4.45 (s, 1H), 4.18−4.12 (m, 1H), 4.11−4.04 (m, 1H), 3.84 (d, J = 11.1 Hz, 1H), 3.76 (dd, J = 11.1, 3.7 Hz, 1H), 3.60−3.52 (m, 1H), 3.48 (dd, J = 13.9, 11.6 Hz, 1H), 3.03−2.94 (m, 2H), 2.70 (s, 3H), 2.48 (s, 3H), 2.45 (s, 3H), 2.43−2.37 (m, 2H),

2.16 (dd, J = 13.1, 7.3 Hz, 1H), 1.97−1.82 (m, 7H), 1.80−1.74 (m, 1H), 1.73 (s, 3H), 1.71−1.62 (m, 2H), 1.56−1.48 (m, 1H), 1.06 (s, 9H). ^{13}C NMR (150 MHz, Methanol-d_4) δ 175.39, 175.31, 173.59, 173.17, 171.88, 171.85, 166.62, 162.69, 157.50, 152.92, 152.17, 149.15, 144.58, 133.39, 133.16, 132.98, 132.69, 132.49, 132.21, 131.71, 131.55, 130.55, 128.29, 115.80, 71.17, 69.85, 60.86, 59.16, 59.07, 58.26, 55.17, 54.56, 49.61, 40.10, 39.12, 38.79, 37.24, 37.22, 36.23, 30.88, 28.16, 27.23, 24.68, 24.47, 15.86, 14.55, 12.98, 11.64. HRMS (ESI) calcd for $C_{50}H_{61}N_9O_6S_2$ [M + H]$^+$ 948.4264, found 948.4263. HPLC purity 97.21%. $[\alpha]_D^{25}$ = +5.6 (c = 1.0 mg/mL, acetone).

(1^6S,12^2S,12^4R,10S,15S,Z)-10-(*tert*-Butyl)-12^4-hydroxy-$1^2$1,$3^1$9-trimethyl-15-(4-(4-methylthiazol-5-yl)phenyl)-1^6H-3-oxa-9,14,21-triaza-1(4,6)-thieno[3,2-*f*][1,2,4]triazolo[4,3-*a*]-[1,4]diazepina-12(1,2)-pyrrolidina-2(1,4)-benzenacyclotricosaphane-8,11,13,22-tetraone (10c). Final compound **10c** was prepared via a similar procedure to that of compound **10a** as a *trans*/*cis* mixture (*trans*/*cis* = 16/1), white solid. ^{1}H NMR (*trans*, 600 MHz, Methanol-d_4) δ 8.87 (s, 1H), 7.50−7.33 (m, 6H), 7.07 (d, J = 9.0 Hz, 2H), 4.88 (dd, J = 9.7, 4.8 Hz, 1H), 4.67 (s, 1H), 4.62−4.56 (m, 2H), 4.43 (s, 1H), 4.13−4.02 (m, 2H), 3.87 (d, J = 11.1 Hz, 1H), 3.74 (dd, J = 11.1, 3.7 Hz, 1H), 3.67−3.60 (m, 1H), 3.49 (dd, J = 14.3, 11.6 Hz, 1H), 3.02 (dd, J = 14.3, 2.4 Hz, 1H), 2.95 (dt, J = 13.7, 7.0 Hz, 1H), 2.70 (s, 3H), 2.48 (s, 3H), 2.45 (s, 3H), 2.44−2.41 (m, 1H), 2.33−2.27 (m, 1H), 2.20−2.15 (m, 1H), 1.93−1.74 (m, 8H), 1.72 (s, 3H), 1.70−1.63 (m, 2H), 1.55−1.47 (m, 3H), 1.05 (s, 9H). ^{13}C NMR (*trans*, 150 MHz, Methanol-d_4) δ 175.73, 173.81, 172.96, 172.02, 166.72, 162.77, 157.54, 152.89, 152.16, 149.11, 145.45, 133.43, 133.11, 132.98, 132.74, 132.50, 132.11, 131.51, 131.43, 130.50, 127.92, 115.90, 71.09, 69.16, 60.63, 59.04, 58.17, 55.00, 54.91, 49.61, 40.80, 39.03, 38.80, 37.95, 36.69, 35.72, 30.55, 28.15, 28.13, 27.49, 27.14, 24.24, 15.85, 14.51, 12.98, 11.63. HRMS (ESI) calcd for $C_{51}H_{63}N_9O_6S_2$ [M + H]$^+$ 962.4421, found 962.4416. HPLC purity 99.05%. $[\alpha]_D^{25}$ = +5.5 (c = 1.0 mg/mL, acetone).

(1^6S,12^2S,12^4R,10S,15S,Z)-10-(*tert*-Butyl)-12^4-hydroxy-$1^2$1,$3^1$9-trimethyl-15-(4-(4-methylthiazol-5-yl)phenyl)-1^6H-3-oxa-9,14,22-triaza-1(4,6)-thieno[3,2-*f*][1,2,4]triazolo[4,3-*a*]-[1,4]diazepina-12(1,2)-pyrrolidina-2(1,4)-benzenacyclotetracosaphane-8,11,13,23-tetraone (10d). Final compound **10d** was prepared via a similar procedure to that of compound **10a** as a *trans*/*cis* mixture (*trans*/*cis* = 7/1), white solid. ^{1}H NMR (*trans*, 600 MHz, Methanol-d_4) δ 8.87 (s, 1H), 7.47−7.36 (m, 6H), 7.02 (d, J = 9.0 Hz, 2H), 4.94−4.88 (m, 1H), 4.64 (s, 1H), 4.61−4.54 (m, 2H), 4.44 (s, 1H), 4.14−4.06 (m, 2H), 3.84 (d, J = 11.2 Hz, 1H), 3.74 (dd, J = 11.1, 3.7 Hz, 1H), 3.57−3.48 (m, 2H), 3.07−3.01 (m, 1H), 2.99 (dd, J = 14.1, 3.0 Hz, 1H), 2.70 (s, 3H), 2.48 (s, 3H), 2.44 (s, 3H), 2.39 (t, J = 6.8 Hz, 3H), 2.19−2.12 (m, 1H), 1.98−1.89 (m, 2H), 1.89−1.78 (m, 6H), 1.71 (s, 3H), 1.68−1.58 (m, 2H), 1.53−1.44 (m, 5H), 1.05 (s, 9H). ^{13}C NMR (*trans*, 150 MHz, Methanol-d_4) δ 175.49, 173.73, 173.14, 172.00, 166.57, 162.78, 157.52, 152.89, 152.17, 149.11, 145.06, 133.42, 133.17, 132.99, 132.66, 132.49, 132.04, 131.53, 130.50, 128.04, 115.69, 71.20, 69.08, 60.93, 59.18, 58.18, 55.07, 54.42, 40.55, 39.03, 38.73, 37.87, 37.07, 36.14, 30.95, 30.25, 28.48, 27.67, 27.20, 27.08, 24.16, 15.85, 14.55, 12.98, 11.64. HRMS (ESI) calcd for $C_{52}H_{65}N_9O_6S_2$ [M + H]$^+$ 976.4577, found 976.4574. HPLC purity 95.97%. $[\alpha]_D^{25}$ = +4.7 (c = 1.0 mg/mL, acetone).

(1^6S,12^2S,12^4R,10S,15S,Z)-10-(*tert*-Butyl)-12^4-hydroxy-12,13,19-trimethyl-15-(4-(4-methylthiazol-5-yl)phenyl)-1^6H-3-oxa-9,14,23-triaza-1(4,6)-thieno[3,2-*f*][1,2,4]triazolo[4,3-*a*]-[1,4]diazepina-12(1,2)-pyrrolidina-2(1,4)-benzenacyclopentacosaphane-8,11,13,24-tetraone (10e). Final compound **10e** was prepared via a similar procedure to that of compound **10a** as a *trans*/*cis* mixture (*trans*/*cis* = 10/1), white solid. ^{1}H NMR (*trans*, 600 MHz, Methanol-d_4) δ 8.86 (s, 1H), 7.46−7.35 (m, 6H), 6.98 (d, J = 9.1 Hz, 1H), 4.90 (dd, J = 10.2, 4.2 Hz, 1H), 4.62 (s, 1H), 4.60−4.54 (m, 2H), 4.44 (s, 1H), 4.11−4.01 (m, 2H), 3.87 (d, J = 11.2 Hz, 1H), 3.75 (dd, J = 11.1, 3.7 Hz, 1H), 3.65−3.59 (m, 1H), 3.48 (dd, J = 14.1, 11.6 Hz, 1H), 3.00 (dd, J = 14.0, 2.6 Hz, 1H), 2.98−2.91 (m, 1H), 2.69 (s, 3H), 2.48 (s, 3H), 2.44 (s, 3H), 2.43−2.39 (m, 1H), 2.38−2.32 (m, 1H), 2.18−2.12 (m, 1H), 1.97−1.90 (m, 1H), 1.88−1.78 (m, 6H), 1.72 (s, 3H), 1.66−1.59 (m, 2H), 1.48−1.41 (m, 8H), 1.07 (s, 9H). ^{13}C NMR (*trans*, 150 MHz, Methanol-d_4) δ 175.74, 173.76, 172.91, 172.10,

166.62, 162.80, 157.49, 152.87, 152.14, 149.08, 145.37, 133.40, 133.12, 132.96, 132.66, 132.47, 131.97, 131.44, 130.47, 127.88, 115.50, 71.16, 68.96, 60.80, 59.29, 58.16, 54.99, 54.69, 40.80, 39.10, 38.77, 38.30, 36.65, 36.02, 31.09, 31.04, 30.84, 28.63, 27.90, 27.19, 27.13, 24.20, 15.86, 15.84, 14.52, 12.99, 11.63. HRMS (ESI) calcd for $C_{53}H_{67}N_9O_6S_2$ [M + H]$^+$ 990.4734, found 990.4732. HPLC purity 98.31%. $[\alpha]_D^{25}$ = +4.9 (c = 1.0 mg/mL, acetone).

(1^6S,12^2S,12^4R,10S,15S,Z)-10-(*tert*-Butyl)-12^4-hydroxy-$1^2$1,$3^1$9-trimethyl-15-(4-(4-methylthiazol-5-yl)phenyl)-1^6H-3-oxa-9,14,24-triaza-1(4,6)-thieno[3,2-*f*][1,2,4]triazolo[4,3-*a*]-[1,4]diazepina-12(1,2)-pyrrolidina-2(1,4)-benzenacyclohexacosaphane-8,11,13,25-tetraone (10f). Final compound **10f** was prepared via a similar procedure to that of compound **10a** as a *trans*/*cis* mixture (*trans*/*cis* = 3/1), white solid. ^{1}H NMR (*trans*, 600 MHz, Methanol-d_4) δ 8.86 (s, 1H), 7.44−7.38 (m, 6H), 6.96 (d, J = 8.8 Hz, 2H), 4.90 (dd, J = 10.0, 4.6 Hz, 1H), 4.60 (s, 1H), 4.59−4.55 (m, 2H), 4.43 (s, 1H), 4.10−4.03 (m, 2H), 3.86 (d, J = 11.2 Hz, 1H), 3.73 (dd, J = 11.1, 3.8 Hz, 1H), 3.60−3.54 (m, 1H), 3.51−3.45 (m, 1H), 3.04−2.97 (m, 2H), 2.69 (s, 3H), 2.48 (s, 3H), 2.44 (s, 3H), 2.41−2.36 (m, 2H), 2.19−2.13 (m, 1H), 1.97−1.88 (m, 1H), 1.87−1.77 (m, 5H), 1.71 (s, 3H), 1.65−1.60 (m, 2H), 1.47−1.38 (m, 10H), 1.05 (s, 9H). ^{13}C NMR (*trans*, 150 MHz, Methanol-d_4) δ 175.72, 173.77, 173.11, 172.13, 166.64, 162.84, 157.52, 152.87, 152.14, 149.09, 145.31, 133.43, 133.11, 132.99, 132.71, 132.47, 131.91, 131.47, 131.44, 130.47, 127.93, 115.46, 71.17, 68.81, 60.83, 58.12, 55.05, 54.56, 40.64, 39.06, 38.78, 38.20, 37.34, 36.69, 36.14, 31.20, 30.85, 30.71, 30.20, 28.85, 28.09, 27.49, 27.22, 27.09, 24.09, 23.03, 15.85, 14.54, 12.98, 11.62. HRMS (ESI) calcd for $C_{54}H_{69}N_9O_6S_2$ [M + H]$^+$ 1004.4890, found 1004.4887. HPLC purity 96.47%. $[\alpha]_D^{25}$ = +5.4 (c = 1.0 mg/mL, acetone).

(1^6S,11^2S,11^4R,9S,14S,Z)-9-(*tert*-Butyl)-11^4-hydroxy-$1^2$1,$3^1$9-trimethyl-14-(4-(4-methylthiazol-5-yl)phenyl)-1^6H-3-oxa-8,13,21-triaza-1(4,6)-thieno[3,2-*f*][1,2,4]triazolo[4,3-*a*][1,4]-diazepina-11(1,2)-pyrrolidina-2(1,4)-benzenacyclotricosaphane-7,10,12,22-tetraone (10g). Final compound **10g** was prepared via a similar procedure to that of compound **10a** as a *trans*/*cis* mixture (*trans*/*cis* = 3/1), white solid. ^{1}H NMR (*trans*, 600 MHz, Methanol-d_4) δ 8.87 (s, 1H), 7.45−7.35 (m, 6H), 7.05 (d, J = 8.9 Hz, 2H), 4.93 (dd, J = 10.0, 4.7 Hz, 1H), 4.61−4.55 (m, 2H), 4.44 (s, 1H), 4.39 (s, 1H), 4.15−4.08 (m, 1H), 4.07−3.98 (m, 1H), 3.86 (d, J = 11.1 Hz, 1H), 3.71 (dd, J = 10.9, 3.8 Hz, 1H), 3.64−3.56 (m, 1H), 3.53−3.46 (m, 1H), 3.06−2.98 (m, 2H), 2.70 (s, 3H), 2.55−2.47 (m, 1H), 2.48 (s, 3H), 2.47−2.41 (m, 4H), 2.16−2.11 (m, 2H), 2.10−2.03 (m, 1H), 1.94−1.87 (m, 1H), 1.85−1.75 (m, 2H), 1.69 (s, 3H), 1.65−1.58 (m, 2H), 1.55−1.44 (m, 6H), 1.00 (s, 9H). ^{13}C NMR (*trans*, 150 MHz, Methanol-d_4) δ 175.52, 173.93, 173.11, 171.94, 166.79, 162.69, 157.50, 152.88, 149.10, 145.26, 133.44, 133.16, 132.97, 132.69, 132.48, 132.32, 131.49, 130.49, 127.97, 115.94, 71.21, 68.42, 60.83, 60.79, 57.96, 55.02, 54.05, 40.18, 39.02, 38.82, 37.73, 36.25, 33.27, 30.67, 29.74, 27.39, 27.21, 27.09, 26.99, 26.47, 15.85, 14.51, 12.97, 11.65. HRMS (ESI) calcd for $C_{51}H_{63}N_9O_6S_2$ [M + H]$^+$ 962.4421, found 962.4418. HPLC purity 99.49%. $[\alpha]_D^{25}$ = +6.7 (c = 1.0 mg/mL, acetone).

(1^6S,13^2S,13^4R,11S,16S,Z)-11-(*tert*-Butyl)-13^4-hydroxy-$1^2$1,$3^1$9-trimethyl-16-(4-(4-methylthiazol-5-yl)phenyl)-1^6H-3-oxa-10,15,23-triaza-1(4,6)-thieno[3,2-*f*][1,2,4]triazolo[4,3-*a*]-[1,4]diazepina-13(1,2)-pyrrolidina-2(1,4)-benzenacyclopentacosaphane-9,12,14,24-tetraone (10h). Final compound **10h** was prepared via a similar procedure to that of compound **10a** as a *trans*/*cis* mixture (*trans*/*cis* = 7/1), white solid. ^{1}H NMR (*trans*, 600 MHz, Methanol-d_4) δ 8.87 (s, 1H), 7.47−7.35 (m, 6H), 6.96 (d, J = 9.0 Hz, 2H), 4.91−4.87 (m, 1H), 4.58−4.53 (m, 3H), 4.43 (s, 1H), 4.10−4.03 (m, 2H), 3.87 (d, J = 11.0 Hz, 1H), 3.75 (dd, J = 11.0, 3.9 Hz, 1H), 3.54−3.45 (m, 2H), 3.08−3.02 (m, 1H), 3.00 (dd, J = 14.0, 2.8 Hz, 1H), 2.69 (s, 3H), 2.48 (s, 3H), 2.44 (s, 3H), 2.37−2.31 (m, 1H), 2.28−2.24 (m, 1H), 2.16−2.11 (m, 1H), 1.96−1.90 (m, 1H), 1.87−1.73 (m, 5H), 1.70 (s, 3H), 1.65−1.61 (m, 2H), 1.54 (p, J = 7.0 Hz, 3H), 1.49−1.41 (m, 6H), 1.06 (s, 9H). ^{13}C NMR (*trans*, 150 MHz, Methanol-d_4) δ 176.29, 176.20, 173.74, 173.66, 173.10, 172.16, 172.14, 166.62, 163.01, 157.53, 152.90, 152.16, 149.12, 145.02, 145.00, 133.42, 133.12, 133.03, 132.73, 132.45, 131.79, 131.55, 131.49, 130.50, 128.08, 115.64, 71.17, 69.32, 60.82, 60.77, 59.70, 59.61, 58.09, 55.14, 54.42, 54.32, 40.32, 39.08, 38.73, 37.67, 37.64, 36.90, 36.86, 36.57, 30.98,

30.02, 29.59, 27.57, 27.22, 27.10, 27.03, 26.87, 26.50, 15.85, 14.51, 12.98, 12.97, 11.62. HRMS (ESI) calcd for $C_{53}H_{67}N_9O_6S_2$ $C_{51}H_{63}N_9O_6S_2$ $[M + H]^+$ 990.4734, found 990.4725. HPLC purity 98.62%. $[\alpha]_D^{25}$ = +5.8 (c = 1.0 mg/mL, acetone).

($1^6S,14^2S,14^4R,12S,17S,Z$)-12-(*tert*-Butyl)-$14^4$-hydroxy-$1,2^1,3^19$-trimethyl-17-(4-(4-methylthiazol-5-yl)phenyl)-1^6H-3-oxa-11,16,24-triaza-1(4,6)-thieno[3,2-f][1,2,4]triazolo[4,3-a]-[1,4]diazepina-14(1,2)-pyrrolidina-2(1,4)-benzenacyclohexacosaphane-10,13,15,25-tetraone (10i). Final compound **10i** was prepared via a similar procedure to that of compound **10a** as a *trans/cis* mixture (*trans/cis* = 16/1), white solid. ^{1}H NMR (*trans*, 600 MHz, Methanol-d_4) δ 8.87 (s, 1H), 7.44 (d, J = 8.3 Hz, 2H), 7.41−7.38 (m, 4H), 6.94 (d, J = 9.0 Hz, 2H), 4.92 (dd, J = 8.9, 5.8 Hz, 1H), 4.67 (s, 1H), 4.59−4.52 (m, 2H), 4.44 (s, 1H), 4.10−4.00 (m, 2H), 3.84 (d, J = 11.2 Hz, 1H), 3.75 (dd, J = 11.1, 3.7 Hz, 1H), 3.54−3.45 (m, 2H), 3.06 (dt, J = 13.2, 7.3 Hz, 1H), 3.00 (dd, J = 14.0, 2.9 Hz, 1H), 2.69 (s, 3H), 2.48 (s, 3H), 2.44 (s, 3H), 2.33−2.28 (m, 2H), 2.16−2.11 (m, 1H), 1.98−1.91 (m, 1H), 1.88−1.72 (m, 5H), 1.70 (s, 3H), 1.67−1.55 (m, 5H), 1.51−1.37 (m, 8H), 1.07 (s, 9H). ^{13}C NMR (*trans*, 150 MHz, Methanol-d_4) δ 175.85, 173.66, 173.07, 172.08, 166.56, 163.02, 157.53, 152.90, 152.16, 149.12, 144.94, 133.40, 133.14, 132.99, 132.69, 132.48, 131.79, 131.57, 131.50, 130.51, 128.10, 115.49, 71.15, 69.14, 60.79, 58.95, 58.17, 55.08, 54.23, 40.51, 39.05, 38.70, 37.67, 36.99, 36.02, 31.05, 30.12, 30.03, 29.03, 27.78, 27.21, 27.10, 26.53, 26.50, 15.86, 14.52, 12.98, 11.63. HRMS (ESI) calcd for $C_{54}H_{69}N_9O_6S_2$ $[M + H]^+$ 1004.4890, found 1004.4889. HPLC purity 98.77%. $[\alpha]_D^{25}$ = +5.5 (c = 1.0 mg/mL, acetone).

Methyl 2-((S)-4-(4-((5-(((S)-1-((2S,4R)-4-Hydroxy-2-((2-hydroxy-4-(4-methylthiazol-5-yl)benzyl)carbamoyl)pyrrolidin-1-yl)-3,3-dimethyl-1-oxobutan-2-yl)amino)-5-oxopentyl)oxy)-phenyl)-2,3,9-trimethyl-6H-thieno[3,2-f][1,2,4]triazolo[4,3-a]-[1,4]diazepin-6-yl)acetate (13). Intermediate **13** was prepared via a Boc-group deprotection from intermediate **11** and a further amide condensation reaction with compound **12**, which was obtained via a deprotection from the intermediate of **4b**. ^{1}H NMR (600 MHz, DMSO-d_6) δ 9.80 (s, 1H), 8.95 (s, 1H), 8.46 (t, J = 6.1 Hz, 1H), 7.91 (d, J = 9.3 Hz, 1H), 7.37 (d, J = 7.8 Hz, 1H), 7.34 (d, J = 8.4 Hz, 2H), 6.95 (d, J = 9.1 Hz, 1H), 6.91 (d, J = 1.8 Hz, 1H), 6.80 (dd, J = 7.8, 1.8 Hz, 1H), 5.12 (d, J = 3.6 Hz, 1H), 4.55 (d, J = 9.3 Hz, 1H), 4.45 (q, J = 7.2 Hz, 2H), 4.35 (s, 1H), 4.28 (dd, J = 16.2, 6.5 Hz, 1H), 4.13 (dd, J = 16.2, 5.4 Hz, 1H), 3.99 (t, J = 6.1 Hz, 2H), 3.68−3.63 (m, 5H), 3.46 (dd, J = 16.5, 6.7 Hz, 1H), 3.39 (dd, J = 16.5, 7.8 Hz, 1H), 2.60 (s, 3H), 2.44 (s, 3H), 2.41 (s, 3H), 2.38−2.29 (m, 1H), 2.25−2.16 (m, 1H), 2.07−1.97 (m, 1H), 1.96−1.87 (m, 1H), 1.74−1.56 (m, 7H), 0.92 (s, 9H). ^{13}C NMR (150 MHz, DMSO-d_6) δ 172.10, 171.76, 171.05, 169.60, 163.43, 160.42, 154.96, 154.64, 151.13, 149.72, 147.30, 131.55, 131.26, 130.47, 130.40, 130.13, 130.03, 129.86, 128.33, 125.26, 119.13, 114.79, 114.05, 68.76, 67.21, 58.53, 56.25, 56.21, 53.05, 51.44, 45.60, 37.81, 37.21, 36.24, 35.12, 34.34, 28.06, 26.26, 21.90, 15.98, 13.94, 12.59, 11.11, 8.52. LC−MS: calcd for $C_{47}H_{56}N_8O_8S_2$ $[M + H]^+$ 925.4, found 925.1.

2-((S)-4-(4-((5-(((S)-1-((2S,4R)-2-((2-((6-((tert-Butoxycarbonyl)amino)hexyl)oxy)-4-(4-methylthiazol-5-yl)-benzyl)carbamoyl)-4-hydroxypyrrolidin-1-yl)-3,3-dimethyl-1-oxobutan-2-yl)amino)-5-oxopentyl)oxy)phenyl)-2,3,9-trimethyl-6H-thieno[3,2-f][1,2,4]triazolo[4,3-a][1,4]diazepin-6-yl)acetic Acid. To stirred solution of intermediate **13** (130 mg, 0.14 mmol, 1.0 equiv) in acetonitrile (10 mL) was added *tert*-butyl (6-bromohexyl)carbamate (57 mg, 0.20 mmol, 1.5 equiv) and K_2CO_3 (56 mg, 0.41 mmol, 3.0 equiv) before being heated to 80 °C for 12 h. The reaction mixture was cooled to RT, filtered and the resulting cake was washed with EtOAc (10 mL). The organic phase was concentrated to give a colorless residue, which was then dissolved in THF/H$_2$O (10 mL, v/v = 2/1). Further LiOH (10 mg, 0.41 mmol, 3.0 equiv) was added. The resulting solution was stirred at RT for 3 h before being concentrated to remove THF. The resulting aqueous phase was acidified (pH 5−6) with 2 N HCl before being extracted with EtOAc (20 mL). The organic phase was dried with anhydrous Na$_2$SO$_4$, filtered, and concentrated to obtain a colorless residue, which was purified by column chromatography (CH$_2$Cl$_2$/MeOH) to obtain intermediate 2-((S)-4-(4-((5-(((S)-1-((2S,4R)-2-((2-((6-((tert-butoxycarbonyl)-

amino)hexyl)oxy)-4-(4-methylthiazol-5-yl)benzyl)carbamoyl)-4-hydroxypyrrolidin-1-yl)-3,3-dimethyl-1-oxobutan-2-yl)amino)-5-oxopentyl)oxy)phenyl)-2,3,9-trimethyl-6H-thieno[3,2-f][1,2,4]-triazolo[4,3-a][1,4]diazepin-6-yl)acetic acid (80 mg, 51% over two steps) as a white solid. ^{1}H NMR (600 MHz, DMSO-d_6) δ 8.98 (s, 1H), 8.46 (t, J = 6.0 Hz, 1H), 7.92 (d, J = 9.3 Hz, 1H), 7.46 (d, J = 7.8 Hz, 1H), 7.35 (d, J = 8.3 Hz, 2H), 6.98 (d, J = 1.7 Hz, 1H), 6.92 (d, J = 9.0 Hz, 2H), 6.89 (dd, J = 7.7, 1.6 Hz, 1H), 6.77 (t, J = 5.8 Hz, 1H), 5.17 (s, 1H), 4.55 (d, J = 9.4 Hz, 1H), 4.48−4.43 (m, 2H), 4.35 (s, 1H), 4.31 (dd, J = 16.7, 6.5 Hz, 1H), 4.14 (dd, J = 16.6, 5.3 Hz, 1H), 4.03 (t, J = 6.3 Hz, 2H), 3.98 (t, J = 6.2 Hz, 2H), 3.70−3.60 (m, 2H), 3.11 (dd, J = 15.2, 6.3 Hz, 1H), 2.94−2.82 (m, 3H), 2.56 (s, 3H), 2.45 (s, 3H), 2.40 (s, 3H), 2.36−2.30 (m, 1H), 2.24−2.17 (m, 1H), 2.06−2.02 (m, 1H), 1.96−1.89 (m, 1H), 1.77−1.59 (m, 9H), 1.46−1.27 (m, 16H), 0.92 (s, 9H). ^{13}C NMR (150 MHz, DMSO-d_6) δ 171.97, 171.77, 169.62, 161.97, 160.11, 156.68, 155.71, 155.46, 151.31, 148.96, 147.65, 131.30, 131.27, 130.61, 130.59, 130.42, 130.04, 130.02, 129.69, 127.51, 126.95, 120.44, 113.91, 111.34, 77.15, 68.75, 67.47, 67.15, 58.57, 56.26, 56.19, 55.36, 37.82, 37.07, 35.11, 34.32, 29.32, 28.54, 28.16, 28.07, 26.25, 25.89, 25.18, 21.88, 15.89, 13.94, 12.58, 11.11. LC−MS: calcd for $C_{57}H_{75}N_9O_{10}S_2$ $[M + H]^+$ 1110.5, found 1110.4.

($1^6S,12^2S,12^4R,10S,Z$)-10-(*tert*-Butyl)-12^4-hydroxy-$1,2^1,3^19$-trimethyl-16^4-(4-methylthiazol-5-yl)-1^6H-3,17-dioxa-9,14,24-triaza-1(4,6)-thieno[3,2-f][1,2,4]triazolo[4,3-a][1,4]diazepina-12(1,2)-pyrrolidina-2(1,4),16(1,2)-dibenzenacyclohexacosaphane-8,11,13,25-tetraone (15a). Final compound **15a** was prepared via a similar procedure to that of compound **10a**, including a Boc-group deprotection and a further amide condensation reaction. **15a** was obtained as a *trans/cis* mixture (*trans/cis* = 7/3), white solid. ^{1}H NMR (*trans/cis*, 600 MHz, Methanol-d_4) δ 8.85 (s, 0.7H), 8.82 (s, 0.3H), 7.39 (d, J = 8.3 Hz, 1.4H), 7.34−7.28 (m, 1.4H), 7.02−6.92 (m, 3.3H), 6.86 (d, J = 1.5 Hz, 0.3H), 6.82 (d, J = 9.0 Hz, 0.6H), 4.64−4.53 (m, 3.3H), 4.50 (s, 0.3H), 4.48 (s, 1.3H), 4.46−4.42 (m, 0.3H), 4.38 (d, J = 14.8 Hz, 0.7H), 4.35 (d, J = 16.0 Hz, 0.3H), 4.11 (t, J = 6.3 Hz, 1.4H), 4.08−3.98 (m, 2.1H), 3.95−3.88 (m, 0.6H), 3.84 (d, J = 11.1 Hz, 0.7H), 3.74 (dd, J = 11.0, 4.1 Hz, 0.7H), 3.71−3.44 (m, 2.8H), 3.11 (dt, J = 13.6, 6.9 Hz, 0.7H), 3.04 (dd, J = 14.5, 2.9 Hz, 0.7H), 3.02−2.97 (m, 0.6H), 2.69 (d, J = 1.4 Hz, 3.0H), 2.47 (s, 2.1H), 2.44 (s, 2.1H), 2.41 (d, J = 2.4 Hz, 2.1H), 2.37−2.17 (m, 2.0H), 2.17−2.11 (m, 1.4H), 1.97−1.87 (m, 2.0H), 1.86−1.73 (m, 4.0H), 1.73−1.60 (m, 7.0H), 1.60−1.51 (m, 2.1H), 1.01 (s, 2.5H), 0.97 (s, 6.5H). ^{13}C NMR (*trans/cis*, 150 MHz, Methanol-d_4) δ 175.92, 175.04, 173.87, 173.81, 173.21, 173.01, 172.63, 172.48, 166.72, 166.69, 162.92, 162.79, 158.52, 157.87, 157.54, 157.51, 152.89, 152.75, 152.19, 152.15, 149.17, 149.10, 133.62, 133.61, 133.26, 133.09, 132.99, 132.90, 132.76, 132.68, 132.66, 132.53, 132.51, 131.90, 131.78, 131.48, 131.31, 130.74, 129.36, 128.03, 128.00, 122.46, 122.41, 115.56, 115.33, 113.43, 113.30, 71.10, 69.52, 69.48, 69.15, 69.08, 68.81, 61.30, 60.71, 59.48, 58.33, 57.89, 55.89, 54.98, 54.93, 41.33, 40.68, 40.52, 39.48, 39.15, 39.10, 38.93, 38.38, 37.46, 36.34, 35.99, 30.63, 30.50, 30.31, 29.46, 28.89, 28.05, 27.85, 27.17, 27.11, 27.06, 27.05, 24.01, 23.57, 15.96, 14.51, 14.47, 12.98, 11.68, 11.62. HRMS (ESI) calcd for $C_{52}H_{65}N_9O_7S_2$ $[M + H]^+$ 992.4527, found 992.4522. HPLC purity 98.87%. $[\alpha]_D^{25}$ = +7.2 (c = 1.0 mg/mL, acetone).

($1^6S,12^2S,12^4R,10S,Z$)-10-(*tert*-Butyl)-12^4-hydroxy-$1,2^1,3^19$-trimethyl-16^4-(4-methylthiazol-5-yl)-1^6H-3,17-dioxa-9,14,25-triaza-1(4,6)-thieno[3,2-f][1,2,4]triazolo[4,3-a][1,4]diazepina-12(1,2)-pyrrolidina-2(1,4),16(1,2)-dibenzenacycloheptacosaphane-8,11,13,26-tetraone (15b). Final compound **15b** was prepared via a similar procedure to that of compound **10a** as a *trans/cis* mixture (*trans/cis* = 7/3), white solid. ^{1}H NMR (*trans/cis*, 600 MHz, Methanol-d_4) δ 8.87 (s, 0.7H), 8.86 (s, 0.3H), 7.39 (d, J = 8.3 Hz, 2H), 7.34 (d, J = 7.7 Hz, 0.7H), 7.23 (d, J = 7.8 Hz, 0.3H), 7.02 (dd, J = 7.7, 1.5 Hz, 0.3H), 6.99 (d, J = 1.3 Hz, 0.7H), 6.98 (dd, J = 7.7, 1.5 Hz, 0.7H), 6.95−6.89 (m, 1.7H), 6.86 (d, J = 9.0 Hz, 0.6H), 4.65−4.60 (m, 0.6H), 4.59−4.52 (m, 2.4H), 4.49−4.43 (m, 1.7H), 4.38 (d, J = 14.5 Hz, 0.7H), 4.30 (d, J = 16.7 Hz, 0.3H), 4.11−3.97 (m, 3.3H), 3.97−3.89 (m, 0.7H), 3.86 (d, J = 10.9 Hz, 0.7H), 3.75 (dd, J = 11.0, 4.1 Hz, 0.7H), 3.71−3.65 (m, 0.3H), 3.65−3.59 (m, 0.6H), 3.56−3.42 (m, 1.7H), 3.21 (q, J = 7.3 Hz, 0.3H), 3.13−3.06 (m, 0.7H), 3.05−3.02 (m, 0.7H), 2.99 (dd, J = 14.0, 2.8 Hz, 0.3H), 2.96−2.91 (m, 0.3H), 2.69 (s,

3.0H), 2.49 (s, 2.1H), 2.46 (s, 0.9H), 2.43 (s, 2.1H), 2.43−2.38 (m, 2.1H), 2.36−2.20 (m, 1.7H), 2.12 (dd, J = 8.3, 4.0 Hz, 1.4H), 1.95−1.89 (m, 1.4H), 1.86−1.72 (m, 5.0H), 1.70 (s, 2.1H), 1.68 (s, 0.9H), 1.67−1.61 (m, 2.1H), 1.60−1.55 (m, 1.4H), 1.51−1.45 (m, 4.6H), 1.01 (s, 2.5H), 0.99 (s, 6.5H). ^{13}C NMR (*trans/cis*, 150 MHz, Methanol-d_4) δ 175.97, 174.82, 173.94, 173.81, 173.13, 172.98, 172.60, 172.52, 166.65, 166.52, 162.94, 162.81, 158.60, 157.83, 157.52, 157.49, 152.91, 152.81, 152.13, 149.17, 149.10, 133.63, 133.59, 133.37, 133.11, 133.07, 133.01, 132.99, 132.71, 132.69, 132.54, 132.49, 132.42, 131.86, 131.64, 131.48, 131.15, 128.29, 128.20, 127.89, 122.44, 122.39, 115.43, 115.24, 113.37, 113.16, 71.08, 69.50, 69.47, 69.16, 69.03, 68.81, 61.36, 60.65, 59.48, 58.26, 57.86, 55.95, 55.14, 55.02, 42.62, 41.43, 40.64, 40.43, 39.55, 39.14, 39.03, 38.36, 37.48, 37.44, 36.24, 36.11, 36.03, 32.79, 31.17, 30.76, 30.69, 30.50, 30.38, 30.37, 30.20, 29.71, 29.32, 29.16, 28.90, 28.17, 28.16, 28.02, 27.19, 27.10, 27.03, 26.90, 24.00, 23.74, 23.46, 23.03, 21.55, 19.87, 19.18, 15.99, 15.97, 14.67, 14.59, 14.51, 14.47, 12.99, 12.98, 11.80, 11.62. HRMS (ESI) calcd for $C_{53}H_{67}N_9O_7S_2$ [M + H]$^+$ 1006.4683, found 1006.4683. HPLC purity 95.35%. $[\alpha]_D^{25}$ = +5.8 (c = 1.0 mg/mL, acetone).

(1^{6}S,12^{2}S,12^{4}R,10S,Z)-10-(*tert*-Butyl)-12^4-hydroxy-1,^{2}1,^{3}1^9-trimethyl-16^4-(4-methylthiazol-5-yl)-1^{6}H-3,17-dioxa-9,14,26-triaza-1(4,6)-thieno[3,2-*f*][1,2,4]triazolo[4,3-*a*][1,4]diazepina-12(1,2)-pyrrolidina-2(1,4),16(1,2)-dibenzenacyclooctacosa-phane-8,11,13,27-tetraone (15c). Final compound **15c** was prepared via a similar procedure to that of compound **10a** as a *trans/cis* mixture (*trans/cis* = 7/3), white solid. ^{1}H NMR (*trans/cis*, 600 MHz, Methanol-d_4) δ 8.86 (s, 0.7H), 8.85 (s, 0.3H), 7.41−7.34 (m, 2H), 7.32 (d, J = 7.6 Hz, 0.7H), 7.25 (d, J = 7.8 Hz, 0.3H), 7.01 (dd, J = 7.8, 1.5 Hz, 0.3H), 6.99−6.95 (m, 1.4H), 6.95−6.89 (m, 1.7H), 6.85 (d, J = 9.0 Hz, 0.6H), 4.65 (d, J = 16.2 Hz, 0.3H), 4.61 (d, J = 9.3 Hz, 0.6H), 4.59−4.55 (m, 1.4H), 4.53 (s, 0.7H), 4.50−4.42 (m, 1.7H), 4.38 (d, J = 15.0 Hz, 0.7H), 4.28 (d, J = 16.2 Hz, 0.3H), 4.12−4.06 (m, 1.4H), 4.05−3.92 (m, 2.7H), 3.87 (d, J = 10.7 Hz, 0.7H), 3.75 (dd, J = 10.9, 4.1 Hz, 0.7H), 3.66−3.61 (m, 0.9H), 3.53−3.44 (m, 2.3H), 3.11−3.04 (m, 1.4H), 3.02−2.96 (m, 0.6H), 2.69 (s, 0.9H), 2.69 (s, 2.1H), 2.48 (s, 2.1H), 2.45 (s, 0.9H), 2.43 (s, 2.1H), 2.42−2.41 (m, 1.2H), 2.40−2.24 (m, 1.7H), 2.22−2.17 (m, 0.3H), 2.15 (dd, J = 8.2, 3.7 Hz, 1.4H), 1.92−1.85 (m, 1.7H), 1.85−1.74 (m, 4.3H), 1.71 (s, 2.1H), 1.67 (s, 0.9H), 1.64−1.55 (m, 3.4H), 1.52−1.39 (m, 6.6H), 1.01 (s, 2.7H), 0.98 (s, 6.3H). ^{13}C NMR (*trans/cis*, 150 MHz, Methanol-d_4) δ 176.03, 174.87, 173.95, 173.87, 173.15, 172.95, 172.65, 172.53, 166.81, 166.65, 162.94, 162.84, 158.48, 157.97, 157.52, 157.51, 152.89, 152.81, 152.16, 152.14, 149.15, 149.13, 133.63, 133.17, 133.11, 133.08, 133.00, 132.75, 132.72, 132.69, 132.52, 132.46, 131.85, 131.73, 131.48, 131.46, 130.53, 128.80, 128.22, 128.03, 122.40, 122.38, 115.44, 115.29, 113.38, 113.27, 71.12, 69.57, 69.41, 69.18, 69.09, 68.78, 66.96, 61.33, 60.70, 59.58, 58.30, 57.89, 57.66, 57.52, 57.38, 56.03, 55.07, 54.98, 41.40, 40.71, 40.60, 39.45, 39.19, 39.14, 38.98, 38.41, 37.46, 36.18, 36.10, 31.06, 30.89, 30.77, 30.71, 30.67, 30.59, 30.53, 30.39, 29.74, 29.25, 28.34, 28.24, 27.48, 27.14, 27.10, 27.03, 23.91, 23.58, 15.96, 15.49, 14.52, 14.49, 12.97, 11.64, 11.62. HRMS (ESI) calcd for $C_{54}H_{69}N_9O_7S_2$ [M + H]$^+$ 1020.4840, found 1020.4834. HPLC purity 99.47%. $[\alpha]_D^{25}$ = +7.7 (c = 1.0 mg/mL, acetone).

Cell Lines. PC-3, HEK293, A549, NCI-H23, MDA-MB-231, and Panc 10.05 cells were purchased from the American Type Culture Collection (ATCC) (Manassas, VA, USA). PC-3, HEK293, and MDA-MB-231 cells were cultured in F-12K medium (Gibco, 21127022), DEME medium (Gibco, C11995500BT), and L-15 medium (Gibco, 11415064), respectively. A549, NCI-H23, and Panc 10.05 cells were cultured in RPMI-1640 medium (Gibco, C11875500BT). PC-3, HEK293, A549, NCI-H23, and Panc 10.05 cells cell lines were grown in the mentioned medium supplemented with 1% penicillin−streptomycin (Gibco, 15070063) and 10% fetal bovine serum (FBS) (ExCell Bio, FSP500). All cells were cultured in a cell incubator at 37 °C in an atmosphere containing 5% (v/v) CO_2, while MDA-MB-231 cells were without CO_2.

Immunoblotting. The process was carried out by following the protocol recommended by Cell Signaling Technology. Briefly, cells were lysed by using SDS lysis buffer [62.5 mM Tris (pH 6.8), 2% SDS, 10% glycerol, 50 mM DTT, 0.01% bromophenol blue]. The lysates were then sonicated on ice for 10 s and heated (100 °C, 10 min), followed by being centrifuged at 4 °C (12000 rpm, 5 min). The denatured proteins in the supernatant were collected and separated by SDS−PAGE gel and subsequently electrophoretically transferred onto polyvinylidene difluoride (PVDF) membranes. The membrane was then incubated in a blocking buffer containing 5% nonfat milk and 0.1% Tween-20 for 1 h at room temperature. The membrane was then incubated with primary antibody overnight at 4 °C followed by 1 h of incubation with secondary antibody. A chemiluminescent signal was detected by using Western Lightning Plus ECL. The protein bands were visualized by an Amersham ImageQuant 800 system. Primary rabbit antibody against Brd4 (ab314432) was purchased from Abcam. Alpha-tubulin (2144s) was purchased from Cell Signaling Technology. Data analysis and statistics were performed using GraphPad Prism 7.0.

TMT Labeled Mass-Spectrometry. *Sample Preparation.* PC-3 cells were seeded in a 6 cm culture dish (2 × 10^6 cells/dish) and cultured for 24 h. Cells were then treated with 100 nM of **SHD913** for 2 h. Subsequently, cells were digested with trypsin and collected by centrifugation (250 g, 5 min). After being washed twice with cold PBS, cells were lysed in 150 μL lysis buffer [0.1% BeyoZonase (Bryotime, D7121), 10 mM HEPES, pH 7.0, 1% SDS, 2 mM MgCl·6H$_2$O]. Cell lysis was quantified using a micro BCA protein assay kit (Thermo Fisher Scientific), and samples were processed and digested using the filter aided sample preparation (FASP) method (600 μg protein/sample), followed by alkylation with iodoacetamide and digestion with trypsin. The samples were then desalted using the Oasis HLB C18 SPE cartridge column (Waters, WAT094225). The collected peptides were lyophilized and reconstituted, and then the peptides were labeled using the TMT 11plex Isobaric Label Reagent Set (Thermo Fisher Scientific) according to the manufacturer's instructions (25 μg/sample). After being labeled, the peptides from 11 samples were pooled together. The pooled TMT 11plex sample was fractionated using high pH reverse-phase chromatography with an XBridge peptide BEH column (130 Å, 3.5 μm, 2.1 × 150 mm, Waters) on an Ultimate 3000 HPLC system (Thermo Scientific/Dionex). Buffers A (10 mM ammonium formate in water, pH 9) and buffer B (10 mM ammonium formate in 90% acetonitrile, pH 9) were used over a linear gradient of 5−60% buffer B over 60 min at a flow rate of 200 μL/min. 48 fractions were collected before concatenation into 12 fractions based on the UV signal of each fraction. All fractions were dried in a concentrator and were reconstituted in 0.2% formic acid solution for MS analysis.

LC-MS/MS Analysis. The fractions were analyzed sequentially on an Orbitrap Fusion Lumos mass spectrometer (Thermo Scientific) coupled with a NanoLC-1200 UHPLC system (Thermo Scientific) using a C18 capillary column. LC separation was using gradient of 6−28% acetonitrile in a 0.2% formic acid solution. The separation flow rate was set up as 250 nL/min. MS3-TMT mass spectrometry methods were modified from the methods reported by the Steven Gygi group.[22] The mass spectrometer was operated in data-dependent mode, and the scan sequence began with an orbitrap MS1 spectrum at resolution 120,000, AGC target 5E5, MaxIT 50 ms. The 20 most intense precursor ions were selected for MS2/MS3 analysis. MS2 analysis consisted of CID and ion trap analysis. Following the acquisition of the MS2 spectrum, the MS3 spectrum was captured with multinotches. MS3 precursors were fragmented by HCD and analyzed with Orbitrap at NCE 65, AGC 1E5, resolution 60,000.

Peptide and Protein Identification. The raw MS data files for all 12 fractions were browsed against the Uniprot-Human-Canonical database by Proteome Discoverer 2.0 for protein identification and TMT reporter ion quantitation. The parameters were set as follows: enzyme used Trypsin/P; maximum number of missed cleavages equal to two; precursor mass tolerance equal to 20 ppm; ion trap fragment mass tolerance was set to 0.6 Da; variable modifications: oxidation (M), acetyl (N-term); fixed modifications: carbamidomethyl (C). The data was filtered by applying a 1% false discovery rate.

Protein Expression and Purification. *Expression of Brd4^{BD2} and Brd3^{BD2} Protein.* A synthetic DNA sequence comprising Brd4^{BD2} (333−460, Uniprot number: O60885) and Brd3^{BD2} (306−416, Uniprot number: Q15059) were cloned into the pET28a vector to express the Brd4^{BD2} fragment with a *N*-terminal hexahistidine (6 × His) and

tobacco etch virus (TEV) cleavage site. Protein was expressed in *Escherichia coli* (*E. coli*) BL21(DE3) cells and cultured in lysogeny broth (LB) medium. Protein expression was induced by 0.4 mM IPTG at 16 °C for 16 h. The BL21(DE3) cells were harvested by centrifugation (6000 rpm, 10 min). The cells were resuspended in lysis buffer [50 mM HEPES, 150 mM NaCl, 1 mM TCEP, 5% glycerol, benzonase, and 1 mM phenylmethylsulfonyl fluoride (PMSF)] and lysed with a high-pressure homogenizer. After centrifugation (18000 rpm, 4 °C, 40 min), the supernatant was loaded on a HisTrap HP column and eluted stepwise with buffer (25 mM HEPES, 300 mM NaCl, 250 mM imidazole, 1 mM TCEP, 5% glycerol). His-tag was removed by TEV protease, and the protein was further purified using the reverse nickel-affinity method. The eluted fractions containing Brd4^{BD2} were pooled, concentrated, and further purified by size exclusion chromatography (SEC) using a Superdex 16/600 75 pg column and stored at −80 °C in storage buffer (25 mM HEPES, 150 mM NaCl, 1 mM TCEP, pH 7.5).

Expression of VHL-ElonginC-ElonginB Protein. The synthetic DNA sequence comprising VHL (55−213, Uniprot number: P40337) was cloned into plasmid pAcycDuet. ElonginC (17−112, Uniprot number: Q15369) was cloned into pRSFDuet and ElonginB (1−118, Uniprot number: Q15370) was cloned into pET32a. The vectors were generously gifted from the Professor Lifeng Pan's Lab (Shanghai Institute of Organic Chemistry). All recombinant proteins were fused with *N*-terminal TRX-His6 follow a HRV 3C cleavage site. Plasmids encoding VHL, ElonginB, and ElonginC were cotransformed into *E. coli* BL21(DE3) cells and cultured in lysogeny broth (LB) medium, containing ampicillin (100 μg/mL), chloramphenicol (30 μg/mL), and kanamycin (34 μg/mL). Protein coexpression was induced by the addition of 0.4 mM IPTG at 16 °C for 16 h. The cells were harvested by centrifugation (6000 rpm, 10 min), and cell pellets were resuspended in lysis buffer [50 mM HEPES, 150 mM NaCl, 1 mM TCEP, 2.5 U/mL benzonase, and 1 mM phenylmethylsulfonyl fluoride (PMSF)] and lysed with a high-pressure homogenizer. After centrifugation (18,000 rpm, 4 °C, 40 min), the supernatant was loaded on a HisTrap HP column and eluted stepwise with buffer (25 mM HEPES, 300 mM NaCl, 250 mM imidazole, and 1 mM TCEP). The fractions containing VCB were pooled, concentrated, and further purified by SEC using a Superdex 26/600 75 pg column and finally collected in elution buffer (25 mM HEPES, 150 mM NaCl, 1 mM TCEP, pH 7.5). The His tags of VCB were removed using 3C protease. The VCB protein was further purified using the reverse nickel-affinity method. Additionally, the VCB protein was purified by anion exchange and size-exclusion chromatography. Finally, the purified VCB protein complexes were stored in a storage buffer [25 mM HEPES, pH 7.5, 150 mM sodium chloride, 1 mM dithiothreitol (DTT)].

Size Exclusion Chromatography. Superdex 75 Increase 16/200 was equilibrated with 25 mM HEPES, 150 mM NaCl, 1 mM TCEP, and pH 7.5 using an AKTA pure micro instrument. A mixture (2 mL) of tagless Brd4 (150 μM), tagless VCB (150 μM), and compound **SHD913** (150 μM, 0.03% DMSO) was then injected into the column, and the sample was eluted at a flow rate of 1 mL/min. UV absorbance was detected at 280 nm.

Bioluminescence Resonance Energy Transfer. The Nano-BRET assay was conducted according to the manufacturer's protocol (Promega). 0.02 μg of Nanoluc-Brd4 vector (Promega, N1691) and 2 μg of HaloTag-VHL vector (Promega, N273A) were combined with 6 μL of FugGENE HD (Promega, E2311) and added into one well of a 6-well culture plate where HEK293 cells had been seeded 1 day in advance and reached 80% confluency. The following day, cells were digested with 0.05% trypsin-EDTA and resuspended in assay buffer (Opti-MEM I Reduced Serum medium, no phenol red, 4% FBS). Cells were then plated in 96-well plates (2×10^5 cells/80 μL/well) in the presence or absence of 0.1 mM HaloTag NanoBRET ligand (Promega, G9801). After 20 h, 10 μL MG-132 was added into each well with a final concentration of 10 μM for 30 min. Cells were then incubated with the test compounds for 2 h. For cell lysis and detection, the NanoBRET Nano-Glo substrate solution (Promega, N1571) was added into the 96-well plate (25 μL/well), and the plate was incubated in darkness while shaking (300 rpm, 1 min). Fluorescence signals were measured using a PerkinElmer Envision Multilabel Reader equipped with a NanoBRET

module (450 nM BP filter and 610 nM LP filter). The wells without Halo ligand served as the background control. The fold increase of fluorescent signal from the compound group compared to those from the DMSO group was plotted against the concentration of the compound using GraphPad Prism 7.0.

Biolayer Interferometry Assay. Purified recombinant Brd4^{BD2} was first biotinylated using the Thermo EZ-link long-chain biotinylation reagent. The Brd4^{BD2} and biotinylation reagent were then mixed in a 1:2 molar ratio in phosphate-buffered saline (PBS) at room temperature for 30 min. Then, the BLI binding assays were performed in 96-well (Greiner 655209) microplates at room temperature while shaking (1000 rpm) using the Octet R8 system (Sartorius). PBS with 0.1% bovine serum albumin (BSA), 0.05% Tween-20, and with or without 0.1% DMSO was used as assay buffer. Biotinylated Brd4^{BD2} protein was tethered on Super Streptavidin (SSA) biosensors (Sartorius) by dipping sensors into 200 μL of protein solutions (50 μg/mL/well). Averagely, a saturation response curve of 6−8 nm was achieved in 10 min. The measurement processes were all under computer control. Data were generated and analyzed by Octet User software. For the initial step, biosensors were washed in an assay buffer for 150 s to form a stable baseline.

1. Binary K_D for Brd4^{BD2}. The biosensors labeled with biotin-Brd4^{BD2} were exposed to the solution containing the compound at the designated concentrations for the association and were monitored for 210 s. The biosensors were then moved back into the assay buffer to disassociate for another 400 s.

2. Ternary K_D for Brd4^{BD2}. The biosensors labeled with biotin-Brd4^{BD2} were exposed to the solution containing the compound and protein complex for the association and were monitored for 210 s (100 μL of 666 nM compound in assay buffer added to 100 μL of 100 ug/mL tagless VCB). The biosensors were then moved back into the assay buffer to disassociate for another 400 s.

3. Intrinsic PPIs between Brd4^{BD2} and VCB. The biosensors labeled with biotin-Brd4^{BD2} were exposed to VCB complex solution for the association and were monitored for 210 s. The biosensors were then moved back into the assay buffer to disassociate for another 400 s.

4. PPIs between Brd4^{BD2} and VCB induced by **SHD913**. The biosensors labeled with biotin-Brd4^{BD2} were exposed to the solution containing 1 μM **SHD913** which had been preincubated with VCB complex for the association and were monitored for 210 s.

Crystallography. Brd4^{BD2}, VCB, and **SHD913** were mixed in a 1:1:1 molar ratio and incubated for 15 min to form a ternary complex with a final protein concentration of 9.5 mg/mL. Crystals were grown using the sitting drop vapor diffuse method consisting of 1 μL of the preincubated protein sample with an equal volume of reservoir solution containing 1.5 M ammonium sulfate, 0.1 M tris base/hydrochloric acid, pH 8.5, 12% (v/v) glycerol at 18 °C. Crystals were obtained after 1 week of incubation. Crystals were cryo-protected using a reservoir solution containing an additional 20% glycerol and flash-frozen in liquid nitrogen. The diffraction data were collected on the BL10U2 beamline at 100 K under a wavelength of 0.97918 using the PIXEL DECTRIS EIGER X 16 M detector in Shanghai Synchrotron Radiation Facility and processed with XDS, pointless and aimless.[24] The complex structure was determined by molecular replacement, employing a reported structure (PDB: 5T35) as a search model, utilizing the program PHASER in the CCP4 suite.[25] SHD913 geometry restraints for refinement were generated using eLBOW.[26] An iterative cycle of refinement was carried out using COOT with PHENIX.[27] Ramachandran plots indicate that 97.58% of backbone torsion angles are in the favored region, 2.30% in the allowed region, and 0.12% in the outlier region. Interfaces observed in the crystal structure were calculated using PISA, and structural figures were generated using PyMOL.[28]

MD Simulations. The complex of structures of Brd4^{BD2}: **SHD913**: VCB, Brd4^{BD2}: **SHD913**, and **SHD913**: VCB was prepared by Protein Preparation Wizard (Schrödinger, LLC, New York, NY, 2021). The SPC model was used for water molecules. The OPLS4 force field was

used for the system. After relaxation, the systems were submitted to 500 ns production simulations. The simulations were run in constant number (N), pressure (P), and temperature (T) (NPT) ensemble at 300 K and 1 atm using Nosé−Hoover and the Martyna-Tobias-Klein algorithm. The RESPA integration method was used with a time step of 2 fs.

Metabolic Stability. The in vitro metabolic stabilities of compounds were assessed by human, mouse and rat liver microsomes, which were prepared and diluted to a final protein concentration of 0.5 mg/mL in a phosphate buffer containing EDTA and MgCl2. The tested compounds were dissolved in DMSO and diluted to a final concentration of 1 μM. The result compound solution was incubated with the microsomes at 37 °C for 5 min, followed by the addition of the NAPH-generating system. The reactions were stopped by using ice-cold acetonitrile at time points of 0, 5, 15, 30, and 45 min. The resulting samples were centrifuged and then analyzed by LC-MS/MS. Ketanserin was selected as the control compound in this assay. The parameters of the results were calculated by the classical formula.

ITC. The titrations were all performed as reverse mode (protein in syringe, ligand in cell) and consisted of 19 injections of 2 μL protein solution (20 mM bis−tris propane, 100 mM NaCl, 1 mM tris(2-carboxyethyl)phosphine (TCEP), pH 7.4) at a rate of 0.5 μL/s at 120 s time intervals. An initial 23 injection (0.4 μL) was made and discarded during data analysis. All experiments were performed at 25 °C while stirring at 600 r.p.m. The compound was diluted from a 5 mM DMSO stock solution to 10 μM in buffer containing 20 mM bis-tris propane, 100 mM NaCl, 1 mM tris(2-carboxyethyl)phosphine (TCEP), pH 7.4. The final DMSO concentration was 0.2%. Bromodomain (in the syringe) was titrated into 1 (in the cell). At the end of the titration, the excess of solution was removed from the cell, the syringe was washed and dried, VCB complex (84 μM, in the same buffer) was loaded in the syringe and titrated into the complex PROTAC−bromodomain.

Titrations for the binary complex Compound−VCB were performed as follows: to the solution of 1 (in the cell), buffer (38.4 μL) was added by means of a single ITC injection. The excess solution was removed from the cell, the syringe was washed and dried, and the VCB complex (in the same buffer) was loaded in the syringe and titrated into the diluted PROTAC solution. The data were fitted to a single-binding-site model to obtain the stoichiometry n, the dissociation constant K_d, and the enthalpy of binding ΔH using the d analyzed using the MicroCal PEAQ-ITC analysis software provided by the manufacturer. Cooperativity (α) values were calculated from the ratio of binary K_d and ternary K_d values determined for VCB binding to compound or compound:bromodomain, respectively.

siRNA. For siRNA transfection, cells were plated in 12-well plates with Pen/Strep-free growth medium overnight. 50 nM of siVHL in 100 μL Opti-MEM was incubated with 2 μL Lipofectamine 2000 in 100 μL Opti-MEM for 15 min at room temperature. Negative Control was only added Lipofectamine 2000. siRNA/Lipofectamine 2000 mix was added to cells slowly. After an 8 hrs incubation, the medium was changed to complete growth medium. Cells were cultured for 72 h for treatment with compounds. The siVHL sense sequence is 5′- GGCUCAA-CUUCGACGGCGA −3′ and the antisense sequence is 5′- UCGCCGUCGAAGUUGAGCC −3′. siNC was just added Lipofect-amine 2000.

Permeability Assay. PC-3 cells were seeded in 6-well dishes for 80−90% confluency and treated with 10 and 30 μM of the indicated compounds for 24 h. The treated cells were washed with PBS 3 times and subsequently lysed with 150 μL of RIPA buffer. The cell lysates were precipitated with acetonitrile and then centrifuged at 2350g for 20 min at 4 °C. The lysate supernatants were collected and subjected to analysis using an LC−MS/MS system. The experiment was conducted by WuXi AppTec. through a research contract.

■ ASSOCIATED CONTENT

Supporting Information

The Supporting Information is available free of charge at https://pubs.acs.org/doi/10.1021/jacsau.4c00831.

Degradation efficiency of compounds **10a−10i** and **15a−15c** in PC-3 cells; degradation efficiency of **SHD913** in PC-3, A549, NCI-H23, MDA-MB-231, and Panc 10.05 cells, degradation efficiency of **MZ1** in PC-3 cells, and intracellular mass of compounds **SHD913**, **MZ1**, **macro-PROTAC-1** per 10^5 cells; **SHD913**: Brd3^{BD2} binary K_d by BLI, and biophysical characterization of PPIs induced by **SHD913** determined by BLI assay; biophysical characterization of PPIs induced by **MZ1**, **SHD913**, and **macroPROTAC-1** determined by ITC assay; super-position of Brd4^{BD2}: **SHD913**: VCB and Brd4^{BD2}: **MZ1**: VCB; 2Fo-Fc electron density map of SHD913 contoured at 1.0 σ; electrostatic surface of the BRD4^{BD2}: **SHD913**: VCB complex; MD simulations for the binary complex of Brd4^{BD2}: **SHD913** or **SHD913**: VCB; ITC data; crystal data collection and refinement statistics; in vitro liver microsomal stabilities of **SHD913** and **MZ1**; and ^{1}H NMR and ^{13}C NMR spectra, and HPLC traces for all final compounds (PDF)

■ AUTHOR INFORMATION

Corresponding Author

Ke Ding − *State Key Laboratory of Chemical Biology, Shanghai Institute of Organic Chemistry, Chinese Academy of Sciences, Shanghai 200032, China;* orcid.org/0000-0001-9016-812X; Email: dingk@sioc.ac.cn

Authors

Chungen Li − *State Key Laboratory of Chemical Biology, Shanghai Institute of Organic Chemistry, Chinese Academy of Sciences, Shanghai 200032, China*

Yihan Chen − *State Key Laboratory of Chemical Biology, Shanghai Institute of Organic Chemistry, Chinese Academy of Sciences, Shanghai 200032, China; University of Chinese Academy of Sciences, Beijing 101408, China*

Weixue Huang − *State Key Laboratory of Chemical Biology, Shanghai Institute of Organic Chemistry, Chinese Academy of Sciences, Shanghai 200032, China*

Yudi Qiu − *Key Laboratory of Structure-Based Drugs Design and Discovery of Ministry of Education, Shengyang Pharmaceutical University, Shenyang 110016, China*

Shengjie Huang − *International Cooperative Laboratory of Traditional Chinese Medicine Modernization and Innovative Drug Discovery of Chinese Ministry of Education (MOE), Guangzhou City Key Laboratory of Precision Chemical Drug Development, College of Pharmacy, Jinan University, Guangzhou 511400, China*

Yang Zhou − *International Cooperative Laboratory of Traditional Chinese Medicine Modernization and Innovative Drug Discovery of Chinese Ministry of Education (MOE), Guangzhou City Key Laboratory of Precision Chemical Drug Development, College of Pharmacy, Jinan University, Guangzhou 511400, China;* orcid.org/0000-0003-4167-6413

Fengtao Zhou − *International Cooperative Laboratory of Traditional Chinese Medicine Modernization and Innovative Drug Discovery of Chinese Ministry of Education (MOE), Guangzhou City Key Laboratory of Precision Chemical Drug Development, College of Pharmacy, Jinan University, Guangzhou 511400, China;* orcid.org/0000-0003-2518-7855

Jian Xu — *Livzon Research Institute, Livzon Pharmaceutical Group Inc., Zhuhai 519000, China*

Xiaomei Ren — *State Key Laboratory of Chemical Biology, Shanghai Institute of Organic Chemistry, Chinese Academy of Sciences, Shanghai 200032, China*

Jinwei Zhang — *State Key Laboratory of Chemical Biology, Shanghai Institute of Organic Chemistry, Chinese Academy of Sciences, Shanghai 200032, China*

Zhen Wang — *State Key Laboratory of Chemical Biology, Shanghai Institute of Organic Chemistry, Chinese Academy of Sciences, Shanghai 200032, China;* ⊙ orcid.org/0000-0001-8762-6089

Ming Ding — *School of Life Science and Technology, China Pharmaceutical University, Nanjing 211198, China*

Complete contact information is available at:
https://pubs.acs.org/10.1021/jacsau.4c00831

Author Contributions

Notes

■ ACKNOWLEDGMENTS

■ ABBREVIATIONS

BLI, biolayer interferometry assay; Brd4^{BD2}, the second bromodomain of Brd4; DBU, 1,8-diazabicyclo[5,4,0]undec-7-ene; DC$_{50}$, the half maximal degradation concentration; DIEA, *N,N*-diisopropylethylamine; DMF, *N,N*-dimethylformamide; DPPA, diphenylphosphoryl azide; Et$_3$N, triethylamine; HATU, 2-(7-azabenzotriazol-1-yl)-*N′,N′,N′*-tetramethyluronium hexafluorophosphate; HPLC, high-performance liquid chromatography; HRMS, high-resolution mass spectra; K$_2$CO$_3$, potassium carbonate; KOH, potassium hydroxide; LC-MS, liquid chromatography—mass spectrometry; LiOH, lithium hydroxide; NanoBRET, nanoluciferase bioluminescence resonance energy transfer; MD, molecular dynamics; NH3.H2O, ammonium hydroxide; NSCLC, non-small cell lung cancer; PEG, polyethylene glycol; PPI, protein—protein interaction; RMSD, root-mean-square deviation; RT, room temperature; SDR, structure-degradation relationship; TFA, trifluoroacetic acid; THF, tetrahydrofuran; TLC, thin-layer chromatography; TPD, targeted protein degradation; VCB, a complex of VHL, Elongin C and Elongin B; VHL, Von Hippel—Lindau protein

■ REFERENCES

(1) (a) Burslem, G. M.; Crews, C. M. Proteolysis-targeting chimeras as therapeutics and tools for biological discovery. *Cell.* **2020**, *181*, 102—114. (b) Békés, M.; Langley, D. R.; Crews, C. M. PROTAC targeted protein degraders: The past is prologue. *Nat. Rev. Drug. Discovery* **2022**, *21*, 181—200. (c) Zhang, C.; Liu, Y.; Li, G.; Yang, Z.; Han, C.; Sun, X.; Sheng, C.; Ding, K.; Rao, Y. Targeting the undruggables - the power of protein degraders. *Sci. Bull.* **2024**, *69*, 1776—1797.

(2) Moreau, K.; Coen, M.; Zhang, A. X.; Pachl, F.; Castaldi, M. P.; Dahl, G.; Boyd, H.; Scott, C.; Newham, P. Proteolysis-targeting chimeras in drug development: a safety perspective. *Br. J. Pharmacol.* **2020**, *177*, 1709—1718.

(3) Dale, B.; Cheng, M.; Park, K. S.; Kaniskan, H.; Xiong, Y.; Jin, J. Advancing targeted protein degradation for cancer therapy. *Nat. Rev. Cancer.* **2021**, *21*, 638—654.

(4) (a) Pettersson, M.; Crews, C. M. Proteolysis targeting chimeras (PROTACs) - past, present and future. *Drug. Discovery Today. Technol.* **2019**, *31*, 15—27. (b) Cao, C.; He, M.; Wang, L.; He, Y.; Rao, Y. Chemistries of bifunctional PROTAC degraders. *Chem. Soc. Rev.* **2022**, *51*, 7066—7114.

(5) Diehl, C. J.; Ciulli, A. Discovery of small molecule ligands for the von Hippel-Lindau (VHL) E3 ligase and their use as inhibitors and PROTAC degraders. *Chem. Soc. Rev.* **2022**, *51*, 8216—8257.

(6) (a) Guerlavais, V.; Sawyer, T. K.; Carvajal, L.; Chang, Y. S.; Graves, B.; Ren, J. G.; Sutton, D.; Olson, K. A.; Packman, K.; Darlak, K.; Elkin, C.; Feyfant, E.; Kesavan, K.; Gangurde, P.; Vassilev, L. T.; Nash, H. M.; Vukovic, V.; Aivado, M.; Annis, D. A. Discovery of sulanemadlin (ALRN-6924), the first cell-permeating, stabilized α-Helical peptide in clinical development. *J. Med. Chem.* **2023**, *66*, 9401—9417. (b) Reddy, D. N.; Ballante, F.; Chuang, T.; Pirolli, A.; Marrocco, B.; Marshall, G. R. Design and synthesis of simplified largazole analogues as isoform-selective human lysine deacetylase inhibitors. *J. Med. Chem.* **2016**, *59*, 1613—1633. (c) Marsault, E.; Peterson, M. L. Macrocycles are great cycles: applications, opportunities, and challenges of synthetic macrocycles in drug discovery. *J. Med. Chem.* **2011**, *54*, 1961—2004. (d) Hill, T. A.; Lohman, R. J.; Hoang, H. N.; Nielsen, D. S.; Scully, C. C.; Kok, W. M.; Liu, L.; Lucke, A. J.; Stoermer, M. J.; Schroeder, C. I.; Chaousis, S.; Colless, B.; Bernhardt, P. V.; Edmonds, D. J.; Griffith, D. A.; Rotter, C. J.; Ruggeri, R. B.; Price, D. A.; Liras, S.; Craik, D. J.; Fairlie, D. P. Cyclic penta- and hexaleucine peptides without N-methylation are orally absorbed. *ACS Med. Chem. Lett.* **2014**, *5*, 1148—1151. (e) Karatas, H.; Li, Y.; Liu, L.; Ji, J.; Lee, S.; Chen, Y.; Yang, J.; Huang, L.; Bernard, D.; Xu, J.; Townsend, E. C.; Cao, F.; Ran, X.; Li, X.; Wen, B.; Sun, D.; Stuckey, J. A.; Lei, M.; Dou, Y.; Wang, S. Discovery of a highly potent, cell-permeable macrocyclic peptidomimetic (MM-589) targeting the WD repeat domain 5 protein (WDR5)-mixed lineage leukemia (MLL) protein-protein interaction. *J. Med. Chem.* **2017**, *60*, 4818—4839.

(7) Jin, L.; Harrison, S. C. Crystal structure of human calcineurin complexed with cyclosporin A and human cyclophilin. *Proc. Natl. Acad. Sci. U.S.A.* **2002**, *99*, 13522—13526.

(8) Liu, J.; Farmer, J. D., Jr.; Lane, W. S.; Friedman, J.; Weissman, I.; Schreiber, S. L. Calcineurin is a common target of cyclophilin-cyclosporin A and FKBP-FK506 complexes. *Cell.* **1991**, *66*, 807−815.

(9) Choi, J.; Chen, J.; Schreiber, S. L.; Clardy, J. Structure of the FKBP12-rapamycin complex interacting with the binding domain of human FRAP. *Science.* **1996**, *273*, 239−242.

(10) Schreiber, S. L. The rise of molecular glues. *Cell.* **2021**, *184*, 3−9.

(11) Schulze, C. J.; Seamon, K. J.; Zhao, Y.; Yang, Y. C.; Cregg, J.; Kim, D.; Tomlinson, A.; Choy, T. J.; Wang, Z.; Sang, B.; Pourfarjam, Y.; Lucas, J.; Cuevas-Navarro, A.; Ayala-Santos, C.; Vides, A.; Li, C.; Marquez, A.; Zhong, M.; Vemulapalli, V.; Weller, C.; Gould, A.; Whalen, D. M.; Salvador, A.; Milin, A.; Saldajeno-Concar, M.; Dinglasan, N.; Chen, A.; Evans, J.; Knox, J. E.; Koltun, E. S.; Singh, M.; Nichols, R.; Wildes, D.; Gill, A. L.; Smith, J. A. M.; Lito, P. Chemical remodeling of a cellular chaperone to target the active state of mutant KRAS. *Science.* **2023**, *381*, 794−799.

(12) Testa, A.; Hughes, S. J.; Lucas, X.; Wright, J. E.; Ciulli, A. Structure-based design of a macrocyclic PROTAC. *Angew. Chem., Int. Ed. Engl.* **2020**, *59*, 1727−1734.

(13) Gadd, M. S.; Testa, A.; Lucas, X.; Chan, K. H.; Chen, W.; Lamont, D. J.; Zengerle, M.; Ciulli, A. Structural basis of PROTAC cooperative recognition for selective protein degradation. *Nat. Chem. Biol.* **2017**, *13*, 514−521.

(14) (a) Filippakopoulos, P.; Qi, J.; Picaud, S.; Shen, Y.; Smith, W. B.; Fedorov, O.; Morse, E. M.; Keates, T.; Hickman, T. T.; Felletar, I.; Philpott, M.; Munro, S.; McKeown, M. R.; Wang, Y.; Christie, A. L.; West, N.; Cameron, M. J.; Schwartz, B.; Heightman, T. D.; La Thangue, N.; French, C. A.; Wiest, O.; Kung, A. L.; Knapp, S.; Bradner, J. E. Selective inhibition of BET bromodomains. *Nature.* **2010**, *468*, 1067−1073. (b) Galdeano, C.; Gadd, M. S.; Soares, P.; Scaffidi, S.; Van Molle, I.; Birced, I.; Hewitt, S.; Dias, D. M.; Ciulli, A. Structure-guided design and optimization of small molecules targeting the protein-protein interaction between the von Hippel-Lindau (VHL) E3 ubiquitin ligase and the hypoxia inducible factor (HIF) alpha subunit with in vitro nanomolar affinities. *J. Med. Chem.* **2014**, *57*, 8657−8663.

(15) Soares, P.; Gadd, M. S.; Frost, J.; Galdeano, C.; Ellis, L.; Epemolu, O.; Rocha, S.; Read, K. D.; Ciulli, A. Group-based optimization of potent and Cell-Active inhibitors of the von Hippel-Lindau (VHL) E3 ubiquitin ligase: structure-activity relationships leading to the chemical probe (2S,4R)-1-((S)-2-(1-Cyanocyclopropa-necarboxamido)-3,3-dimethylbutanoyl)-4-hydroxy-N-(4-(4-methyl-thiazol-5-yl)benzyl)pyrrolidine-2-carboxamide (VH298). *J. Med. Chem.* **2018**, *61*, 599−618.

(16) Castellani, B.; Eleuteri, M.; Bona, S. D.; Cruciani, G.; Desantis, J.; Goracci, L. VHL-modified proteolysis targeting chimeras (PROTACs) as a strategy to evade metabolic degradation in in vitro applications. *J. Med. Chem.* **2023**, *66*, 13148−13171.

(17) Anderson, K. W.; Ikawa, T.; Tundel, R. E.; Buchwald, S. L. The selective reaction of aryl halides with KOH: synthesis of phenols, aromatic ethers, and benzofurans. *J. Am. Chem. Soc.* **2006**, *128*, 10694−10695.

(18) Kofink, C.; Trainor, N.; Mair, B.; Wöhrle, S.; Wurm, M.; Mischerikow, N.; Roy, M. J.; Bader, G.; Greb, P.; Garavel, G.; Diers, E.; McLennan, R.; Whitworth, C.; Vetma, V.; Rumpel, K.; Scharnweber, M.; Fuchs, J. E.; Gerstberger, T.; Cui, Y.; Gremel, G.; Chetta, P.; Hopf, S.; Budano, N.; Rinnenthal, J.; Gmaschitz, G.; Mayer, M.; Koegl, M.; Ciulli, A.; Weinstabl, H.; Farnaby, W. A selective and orally bioavailable VHL-recruiting PROTAC achieves SMARCA2 degradation in vivo. *Nat. Commun.* **2022**, *13*, 5969.

(19) Shunatona, H. P.; Shearn-Nance, G. P.; Mitchell, S. A.; Buell, J. Bifunctional degraders of hematopoietic progenitor PROGENITOR kinase and therapeutic uses thereof. WO2021226262A1, 2021.

(20) (a) Luo, H.; Yin, H.; Tang, C.; Wang, P.; Liang, F. Synthesis of cyclic peptide reniochalistatin E and conformational isomers. *Chin. Chem. Lett.* **2018**, *29*, 1143−1146. (b) Qiu, R.; Li, X.; Huang, K.; Bai, W.; Zhou, D.; Li, G.; Qin, Z.; Li, Y. Cis-trans isomerization of peptoid residues in the collagen triple-helix. *Nat. Commun.* **2023**, *14*, 7571. (c) Rüdisser, S. H.; Matabaro, E.; Sonderegger, L.; Güntert, P.; Künzler, M.; Gossert, A. D. Conformations of macrocyclic peptides sampled by nuclear magnetic resonance: models for cell-permeability. *J. Am. Chem. Soc.* **2023**, *145*, 27601−27615.

(21) Shergalis, A. G.; Marin, V. L.; Rhee, D. Y.; Senaweera, S.; McCloud, R. L.; Ronau, J. A.; Hutchins, C. W.; McLoughlin, S.; Woller, K. R.; Warder, S. E.; Vasudevan, A.; Reitsma, J. M. CRISPR screen reveals BRD2/4 molecular glue-like degrader via recruitment of DCAF16. *ACS. Chem. Biol.* **2023**, *18*, 331−339.

(22) Liu, S.; Tong, B.; Mason, J. W.; Ostrem, J. M.; Tutter, A.; Hua, B. K.; Tang, S. A.; Bonazzi, S.; Briner, K.; Berst, F.; Zécri, F. J.; Schreiber, S. L. Rational screening for cooperativity in small-molecule inducers of protein-protein associations. *J. Am. Chem. Soc.* **2023**, *145*, 23281−23291.

(23) (a) Eugene, F. D., Jr.; Chad, J. M. G.; Sparer, H. S.; David, A. S. A comprehensive mathematical model for Three-Body binding equilibr. *J. Am. Chem. Soc.* **2013**, *135*, 6092. (b) Casement, R.; Bond, A.; Craigon, C.; Ciulli, A. Mechanistic and structural features of PROTAC ternary complexes. *Methods Mol. Biol.* **2021**, *2365*, 79−113.

(24) (a) Kabsch, W. XDS. *Acta Crystallogr. D* **2010**, *66*, 125−132. (b) Evans, P. R. An introduction to data reduction: space-group determination, scaling and intensity statistics. *Acta Crystallogr. D* **2011**, *67*, 282−292. (c) Evans, P. R.; Murshudov, G. N. How good are my data and what is the resolution? *Acta Crystallogr. D* **2013**, *69*, 1204−1214.

(25) (a) McCoy, A. J.; Grosse-Kunstleve, R. W.; Adams, P. D.; Winn, M. D.; Storonia, L. C.; Reada, R. J. Phaser crystallographic software. *J. Appl. Crystallogr.* **2007**, *40*, 658−674. (b) Agirre, J.; Atanasova, M.; Bagdonas, H.; Ballard, C. B.; Baslé, A.; Beilsten-Edmands, J.; Borges, R. J.; Brown, D. G.; Burgos-Mármol, J. J.; Berrisford, J. M.; Bond, P. S.; Caballero, I.; Catapano, L.; Chojnowski, G.; Cook, A. G.; Cowtan, K. D.; Croll, T. I.; Debreczeni, J. É.; Devenish, N. E.; Dodson, E. J.; Drevon, T. R.; Emsley, P.; Evans, G.; Evans, P. R.; Fando, M.; Foadi, J.; Fuentes-Montero, L.; Garman, E. F.; Gerstel, M.; Gildea, R. J.; Hatti, K.; Hekkelman, M. L.; Heuser, P.; Hoh, S. W.; Hough, M. A.; Jenkins, H. T.; Jiménez, E.; Joosten, R. P.; Keegan, R. M.; Keep, N.; Krissinel, E. B.; Kolenko, P.; Kovalevskiy, O.; Lamzin, V. S.; Lawson, D. M.; Lebedev, A. A.; Leslie, A. G. W.; Lohkamp, B.; Long, F.; Malý, M.; McCoy, A. J.; McNicholas, S. J.; Medina, A.; Millán, C.; Murray, J. W.; Murshudov, G. N.; Nicholls, R. A.; Noble, M. E. M.; Oeffner, R.; Pannu, N. S.; Parkhurst, J. M.; Pearce, N.; Pereira, J.; Perrakis, A.; Powell, H. R.; Read, R. J.; Rigden, D. J.; Rochira, W.; Sammito, M.; Rodríguez, F. S.; Sheldrick, G. M.; Shelley, K. L.; Simkovic, F.; Simpkin, A. J.; Skubak, P.; Sobolev, E.; Steiner, R. A.; Stevenson, K.; Tews, I.; Thomas, J. M. H.; Thorn, A.; Valls, J. T.; Uski, V.; Usón, I.; Vagin, A.; Velankar, S.; Vollmar, M.; Walden, H.; Waterman, D.; Wilson, K. S.; Winn, M. D.; Winter, G.; Wojdyr, M.; Yamashita, K. The CCP4 suite: integrative software for macromolecular crystallography. *Acta Crystallogr. D* **2023**, *79*, 449−461.

(26) Moriarty, N. W.; Grosse-Kunstleve, R. W.; Adamsa, P. D. Electronic ligand builder and optimization workbench (eLBOW): a tool for ligand coordinate and restraint generation. *Acta Crystallogr. D* **2009**, *65*, 1074−1080.

(27) (a) Emsley, P.; Cowtan, K.; Evans, P. R.; Murshudov, G. N. Howgoodaremydataandwhatistheresolution? *Acta Crystallogr. D* **2014**, *60*, 2126−2132. (b) Adams, P. D.; Afonine, P. V.; Bunkóczi, G.; Chen, V. B.; Davis, I. W.; Echols, N.; Headd, J. J.; Hung, L.; Kapral, G. J.; Grosse-Kunstleve, R. W.; McCoy, A. J.; Moriarty, N. W.; Oeffner, R.; Read, R. J.; Richardson, D. C.; Richardson, J. S.; Terwilliger, T. C.; Zwart, P. H. PHENIX: a comprehensive python-based system for macromolecular structure solution. *Acta Crystallogr. D* **2010**, *66*, 213−221.

(28) Krissinel, E.; Henrick, K. Inference of macromolecular assemblies from crystalline state. *J. Mol. Biol.* **2007**, *372*, 774−797.